Atmospheric Deposition of Biologically Relevant Trace Metals in the Eastern Adriatic Coastal Area

Abra Penezić[a]*, Andrea Milinković[a], Saranda Bakija Alempijević[a], Silva Žužul[b], Sanja Frka[a]*

[a]Division for Marine and Environmental Research, Ruđer Bošković Institute, Zagreb, Croatia

[b]Institute for Medical Research and Occupational Health, Zagreb, Croatia

*Corresponding authors: Abra Penezić abra@irb.hr; Sanja Frka frka@irb.hr

Abstract

Aerosol (PM_{10}), bulk deposition, sea surface microlayer (SML) and underlying water (ULW) samples were collected simultaneously during a field campaign at the middle Adriatic coastal site between February and July 2019, to assess the impact of atmospheric deposition (AD) of biologically relevant trace metals (TM) (Zn, Cu, Co, Ni, Cd and Pb) on the sea surface responses in an oligotrophic coastal region. Anthropogenic emissions from continental Europe, alongside local/regional domestic heating, likely affected the concentrations of Zn, Cd and Pb in aerosols during winter-early spring, while traffic emissions during the tourist season impacted Ni, Co and Cu aerosol concentrations. Additionally, open-fire biomass burning (BB) episodes caused considerable TM concentration increases, while Saharan dust intrusion in spring led to a 10-fold increase in Co concentrations in PM_{10} samples. These intensive episodes significantly affected the bulk deposition fluxes of TMs, showing that a small number of such extreme events, common to Mediterranean coastal areas, could be responsible for most of the AD. Enrichments and concentrations of total TMs in SML samples collected following BB events

indicated that such events, along with high precipitation, influenced TM partitioning in surface water layers. We estimated that AD represents a significant source of TM to the shallow middle Adriatic coastal area, highlighting the need to further explore the atmosphere-sea surface links, to expand our understanding of the biogeochemistry of these important micronutrients and pollutants, including their impact on the aquatic community.

1. Introduction

Atmospheric deposition (AD) is recognized as a significant, and in some cases dominant, pathway by which anthropogenic and natural material is transported from the continent to coastal and open seas (Guerzoni et al., 1999). Once deposited through dry and wet processing, atmospheric aerosols provide the aqueous ecosystems with an external source of typical macro (N and P) and micronutrients (Fe), but also trace metals (TM) such as Zn, Co, Ni, Cd, Cu, Pb and Mn, whose importance is being acknowledged due to their impact on marine organisms (Baker et al., 2016; Bonnet and Guieu, 2006; Browning et al., 2017; Desboeufs et al., 2018; Hassler et al., 2012; Mahowald et al., 2018). TMs are essential to the aquatic microbial community as they limit or co-limit phytoplankton growth, act as enzymatic co-factors in various biochemical cycles, and participate in the uptake and metabolism processes of nitrogen, silicate, carbon, and phosphate (Lee et al., 1995, Morel and Price, 2003).

The AD influx of TMs may be particulary important for oligotrophic environments, which account for up to 60% of the global ocean (Maranon et al., 2003). The Mediterranean Sea is a semi-enclosed oligotrophic sea that is under constant influence of anthropogenic and natural emissions brought by air masses from Europe, Africa and Asia (Kanakidou et al., 2011) and also receives the highest rate of aeolian material in the global ocean (Guerzoni et al., 1999).

An important source of crust-dominated aerosols containing macro- and micronutrients such as P, Fe, Zn, is Saharan dust, which is transported to the Mediterranean basin mainly in spring and summer in the form of non-continuous dust pulses, (Guieu et al., 2002; Guerzoni et al., 1997; Ridame et al., 1999). Despite the general paradigm that TMs from anthropogenic material are more soluble compared to those from lithogenic material, there are large uncertainties associated with TM solubility in atmospheric deposition and in marine surface waters (Baker et al., 2016; Chance et al., 2015; Fishwick et al., 2018, Mahowald et al. 2018), implying a potentially significant impact of dust TMs on the biogeochemistry of Mediterranean surface waters.

The number of biomass burning (BB) events from wildfires increased drastically in recent decades throughout the Mediterranean area, causing severe economic and environmental damage (Pausas et al., 2004). Estimates of future climate change impacts suggest that the burned area and carbon emissions from BB will increase, particularly in the Mediterranean basins, the Balkan regions and Eastern Europe (Migliavacca et al., 2013). Consequently, external AD inputs should become even more important for oligotrophic Mediterranean regions with increased aerosol loads, including plumes of Saharan desert dust (Moulin et al., 1997) and a shallower mixed layer depth, due to increasing temperatures.

The majority of data related to AD impacts generated in the Mediterranean so far have been conducted in its western and eastern regions (e.g., Desboeufs et al., 2018, Eker-Develi et al., 2006, Guieu et al., 2010, Heimburger et al., 2010), while only a limited number of studies are related to the Adriatic Sea sub-basin, and are generally restricted to its northern part (Contini et al., 2012, Rossini et al., 2001, 2005, Čačković et al., 2009). The Adriatic Sea is under the combined influence of local, regional and long-distance sources of natural and anthropogenic emissions. North Adriatic is considered one of the most eutrophic parts of the Mediterranean due to strong riverine inputs (Milliman et al., 2016, Siokou-Frangou et al., 2010). In contrast,

the middle and southern Adriatic present oligotrophic regions (Milliman et al., 2016, Cukrov et al., 2008, Ljubešić et al., 2007), where AD is expected to significantly affect primary production (Richon et al., 2017, Richon et al., 2018). Oligotrophic Adriatic regions are impacted by Mediterranean arid conditions with frequent transport of Saharan dust, and similar to the rest of the Mediterranean, exhibit a high to very high risk of wildfires during summer (Bakšić et al., 2015), effects of which remain unexplored.

AD onto the sea surface cannot be completely understood without considering the interfacial processes within the sea surface microlayer (SML). The SML is the top 1000 µm of the sea surface, governing all exchange processes between the atmosphere and the sea. It is a unique environmental niche, described as a gelatinous film that provides a home for complex microbial community (Cunliffe and Murrell, 2009, Stolle et al., 2020). The accumulation of organic matter (OM) in the SML facilitates the accumulation of TMs through complexation with organic ligands and physical interactions with particulate matter (Cunliffe et al., 2010, 2013, Hunter and Liss, 1981). There are many strategies that microorganisms use to successfully uptake TMs under TM-limiting conditions as well as mitigate the detrimental effects of increased TM concentrations. This is particularly demanding within the SML, where the interconnections between physical, biological and chemical processes such as AD impacts, OM production, (photo)transformation and degradation become especially relevant and are still surprisingly poorly characterized (Bakker et al., 2016; Engel et al., 2017; Mahowald et al., 2018; Stolle et al., 2020). A better understanding of the increasingly important processes affecting the air-water region can only be achieved through studies that consider both atmospheric and sea surface compartments as an integrated whole (Engel et al., 2017).

Therefore, this study focused on the AD impacts of biologically relevant trace metals (Zn, Cu, Co, Ni, Cd and Pb) on the complex sea surface responses of an oligotrophic coastal region, considering the SML at the air-water interface. A comprehensive dataset, comprising TM

concentrations in ambient aerosol particles, bulk deposition and sea surface, differentiating between the SML and underlying water, was obtained during a field campaign conducted from February to July 2019 on the middle Adriatic coastal site. This study aimed to: (i) provide new insights into the variability of aerosol TM levels in relation to different seasons, air-mass impacts and special events, such as open-fire BB emissions and Saharan dust inputs typical of the coastal Mediterranean area, (ii) identify the magnitude and temporal variability of atmospheric TM deposition fluxes to the coastal region, (iii) better understand the controlling factors and processes that can impact TM concentrations and enrichments at the air-water interface in the coastal environments. To the best of our knowledge, this work is the first study of its kind ever conducted in the Adriatic Sea area and paves the way to a better understanding of the linkage between the ocean and the atmosphere. Knowledge of the interactions between different environmental compartments, taking into account the role of environmental interfaces, represents a fundamental feature for understanding the impacts of various pressures on the environment in general.

2. Materials and methods

2.1. Site description

Sampling of marine and atmospheric samples was conducted during the field campaign of BiREADI project, in the period from February 7th to July 10th 2019 at the coastal zone of the Šibenik archipelago at the middle Adriatic coastal area (Fig. 1). The sampling of the marine samples was performed along a 2 km long transect offshore of the small settlement of Jadrija (Fig. 1, red line) while atmospheric sampling was conducted 2 km inland from the marine transect area, at a rural site Martinska (43°73′ N, 15°87′ E) (Fig. 1, blue dot). The study area

125 presents a coastal oligotrophic zone with low influence of the nearby Krka River runoff, while
126 the city of Šibenik (population ~34 000) is the only source of direct anthropogenic
127 eutrophication (Gržetić et al., 1991; Legović et al., 1994). Lower reach of Krka River estuary
128 is located about 3 km SE from the sampling transect and the general water circulation carries
129 the water from the Šibenik Bay area towards the S and SE direction, i.e. away from our study
130 zone. The region is generally characterized by extensive tourism and mariculture. The climate
131 is Mediterranean, with mild, wet winters and warm to hot, dry summers, and the middle Adriatic
132 coastal area is permanently exposed to from high to very high fire risk, with a long history of
133 extreme forest fires (Šiljković and Mamut, 2016).
134

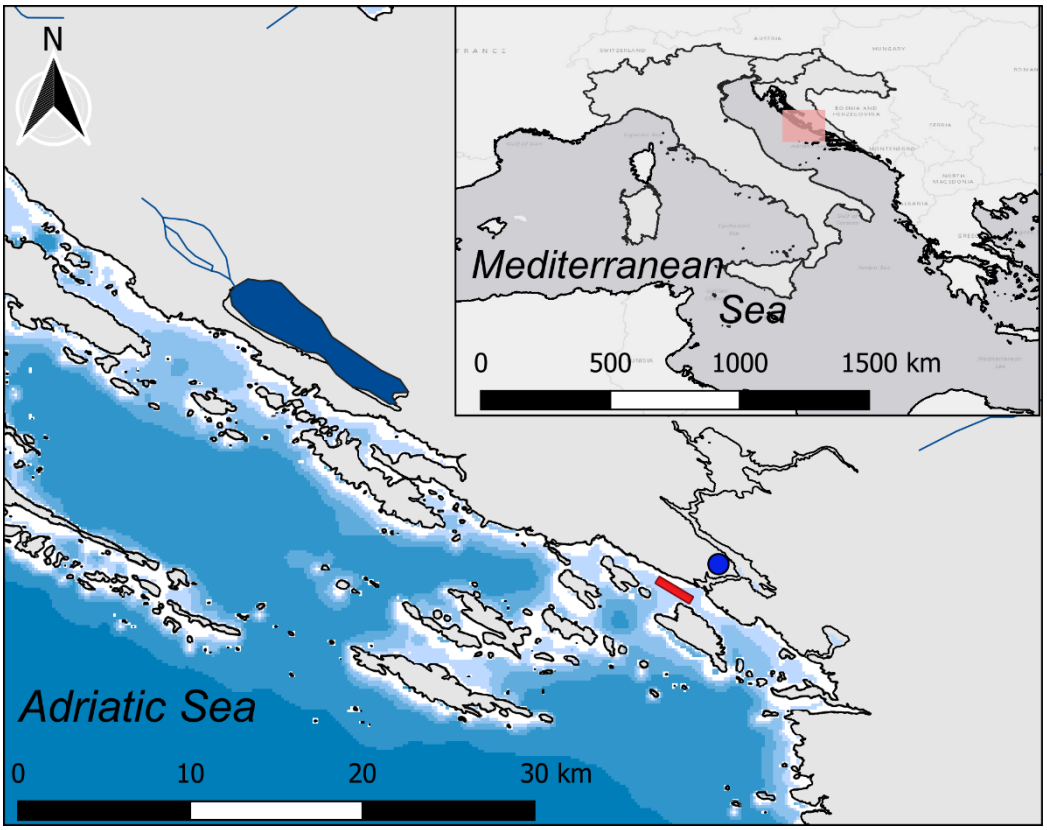

135
136
137 **Fig. 1.** Sampling area on the coastal middle Adriatic area, Croatia. The seawater sampling
138 transect and the atmospheric sampling site are marked with a red line and a blue dot,
139 respectively.

2.2. Marine sample collection and analysis

The SML was collected using an in-house constructed rotating drum sampler operated by an electromotor from on board a rubber auxiliary boat propelled by an electric engine, to prevent contaminations. The sampling cylinder (40 cm diameter) was made of poly(methyl)methacrylate (PMMA). Before use the cylinder was cleaned with 10% hydrochloric acid (p.a., Merck, Darmstadt, Germany) and rinsed with deionized ultrapure Milli-Q water (Millipore, Billerica, USA). Prior to each sampling, the sampler was operated for at least 15 minutes to ensure thorough rinsing with seawater. Samples were collected by a PTFE/PC wiper directly into plastic bottles (fluoropolymer Nalgene FEP) cleaned with nitric acid and Milli-Q water for TM analysis and into glass bottles washed with chromic-sulfuric acid for OM analysis. Both were rinsed two to three times with the sample before collection. The thickness of the sampled SML (20 ± 3 µm) was calculated using the dimensions of the rotating cylinder, the number of rotations and the volume of sample collected. The ULW samples were collected from 1 m depth parallel to the SML along the same transect directly into acid cleaned FEP/glass sampling bottles.

2.2.1. Trace metals in marine samples

Samples for determining dissolved TM concentrations in the SML and ULW were first filtrated using a syringe 0.45 µm cellulose nitrate membrane filters (Sartorius) into FEP bottles and then acidified to pH ≤ 2 with nitric acid (Suprapur®, Merck, Darmstadt, Germany). Unfiltered samples were acidified to pH ≤ 2 with nitric acid. All samples were then UV-irradiated (150 W mercury lamp, Hanau, Germany) for 24 to 48 hours to remove naturally

present OM (Omanović et al., 2006). The concentration of TMs in the unfiltered acidified samples represents the acid-leachable, quasi-total concentration of TMs, but will be referred to as total TM concentrations throughout the text (Cindrić et al., 2015; Cuculić et al., 2009; Cukrov et al., 2008). TM concentrations were obtained by voltammetry using the ECO Chemie μAUTOLAB multimode potentiostat (Utrecht, The Netherlands) connected to a three-electrode Metrohm 663 VA STAND system (Herissau, Switzerland). A hanging mercury drop was used as a working electrode. Cu, Cd, Pb and Zn concentrations were determined by differential pulse anodic stripping voltammetry (DPASV) and Ni and Co by adsorptive cathodic stripping voltammetry (ACSV), with standard additions. Most important experimental parameters are provided in Table S1. The limits of quantification (LOQ) obtained in acidic Milli-Q water were 1, 2, 5, 10 ng L^{-1} for Cd, Pb, Cu and Zn, respectively, and 1 and 10 ng L^{-1} for Co and Ni, respectively. The accuracy of the voltammetric methods used was tested using a seawater reference material for trace metals (NASS-6), and all measured metal concentrations were within the reported certified values (Table S2).

2.2.2. Organic matter in marine samples

Seawater samples were analysed for dissolved (DOC) and particulate organic carbon (POC) according to the methods EN 1484:2002 in a laboratory accredited according to the HRN EN ISO/IEC 17025:2017 standard. Seawater aliquots were filtrated using glass fibre filters (GF/F 0.7 μm Whatman, Maidestone, UK) precombusted for 4 h at 450 °C, in an all-glass filtering system (Millipore, Billerica, USA). For POC analysis, GF/F filters containing samples were stored at -80 °C until analysed. Filtrates for DOC analysis were collected in duplicates into 22 mL glass vials which were previously washed with chromic-sulfuric acid, rinsed with Milli-Q water and precombusted at 450 °C for 4 h. Samples were preserved with $HgCl_2$ (final

concentration 10 mg L^{-1}) and stored in the dark at 4 °C until analysis. For DOC measurements, a TOC-VCPH analyser (Shimadzu) with platinum silica catalyst and non-dispersive infrared (NDIR) detector for CO_2 measurements was used. Concentration was calculated as the average of 3 – 5 replicates. The average instrument and Milli-Q blank correspond to 0.03 mg L^{-1} (n = 33) with high reproducibility (1.6%). POC was analysed with a solid sample module SSM-5000A associated to the Shimadzu TOC-VCPH analyser calibrated with glucose. After acidification with hydrochloric acid (2 M) to remove the inorganic carbonate fraction, the filters were dried for 12 h at 50 °C. The samples were combusted in a flow of oxygen at 900 °C, and the produced CO_2 was detected by an NDIR detector. POC concentrations were corrected based on the blank filter measurements. The average instrument and Milli-Q blanks correspond to 0.005 mg L^{-1}. The reproducibility determined using a glucose standard was 3%.

2.3. Atmospheric sample collection and analysis

PM_{10} samples were collected continuously as 48-h samples on Pallflex membrane quartz fibre filters (Pall Life Sciences, Port Washington, New York) using a low-volume automatic sampler PNS 18T-DM-3.1 (Comde-Derenda, Stahnsdorf, Germany) mounted on top of the sampling station (~10 m above ground level (a.g.l)), at a flow rate of 2.3 m^3 h^{-1}. After sampling, one half of each filter was used for TM analysis. Operational blank filters were processed in the same way as the collected samples, but without air exposure. Bulk deposition samples were collected with a Bergerhoff collector into HDPE bottles cleaned with nitric acid according to EN 15841:2009 Standard. Samples containing total wet and dry deposition were collected at 2-week intervals.

2.3.1. Trace metals in atmospheric samples

The PM_{10} samples and bulk deposition samples were analysed for Cd, Pb and Ni according to the methods EN 14902:2005 and EN 15841:2009 in a laboratory accredited for these methods according to the HRN EN ISO/IEC 17025:2017 Standard. The same protocols and quality control assurance were applied for sample preparation and analysis of Cu, Zn and Co. PM_{10} samples were digested with nitric acid (65% p.a. Merck) in an UltraCLAVE digestion system (Milestone Srl, Italy) using an application note for paper filter digestion (maximum temperature 240 °C, maximum pressure 130 bar and maximum microwave power 1000 W). Bulk deposition samples were quantitatively transferred to an evaporating dish, passing through a plastic screen (mesh size ~1 mm). Samples were evaporated to dryness, mixed with nitric acid and transferred into the digestion vessel for UltraCLAVE. The samples were further digested in the same way as PM_{10} samples. All solutions of the atmospheric samples were analysed by inductively coupled plasma mass spectrometry (ICP-MS 7500cx, Agilent Technologies, Waldbroon, Germany). Collision mode with helium gas was used to remove the interferences. A solution containing Sc, Ge, Rh, Lu and Bi was added to all samples as an internal standard. Several certified reference materials (ERM CZ-120, NIST 1648a) were analysed each time along with samples as part of a quality control protocol. Recovery rates ranged within ± 10% of the certified values(Table S2).

2.4. Meteorology and air-mass backward trajectories analysis

Air temperature, air pressure, wind speed and direction were recorded at the Martinska station during the sampling campaign. The daily average temperature, wind speed and measured daily precipitation are presented in Fig. 2. Following a distinct seasonal pattern, the coldest sampling month was February (8.7 ± 1.8 °C), while the maximum temperature was reached in

June – July period (27.4 ± 2.9 °C). Precipitation was highly variable during the investigated period with a mean value of 16.6 ± 11.0 mm. February was characterized by a minimum total rainfall of 2.5 mm, while the observed monthly mean precipitation maximum during the April – May period (21.4 ± 8.8 mm) was typical for the area. According to the Croatian Meteorological and Hydrological Service, in 2019 the Šibenik area was characterized by above-average annual precipitation, and above average annual air temperature compared to a multi-year average (1981 – 2010) (https://meteo.hr/klima_e.php?section=klima_pracenje&param=ocjena&MjesecSezona=godina&Godina=2019, accessed January 10th, 2021). The average wind speed during the study period was 6.0 ± 4.5 m s^{-1}, with strong N to N/NE Bora winds (over 15 m s^{-1}) blowing from the mountainous region to the sea prevailing during the winter and early spring months. Southerly winds (up to 10 m s^{-1} on average) blowing from the sea were also generally frequent, especially from March to July. Generally, a decrease in wind speed was observed from February towards summer (Fig. 2).

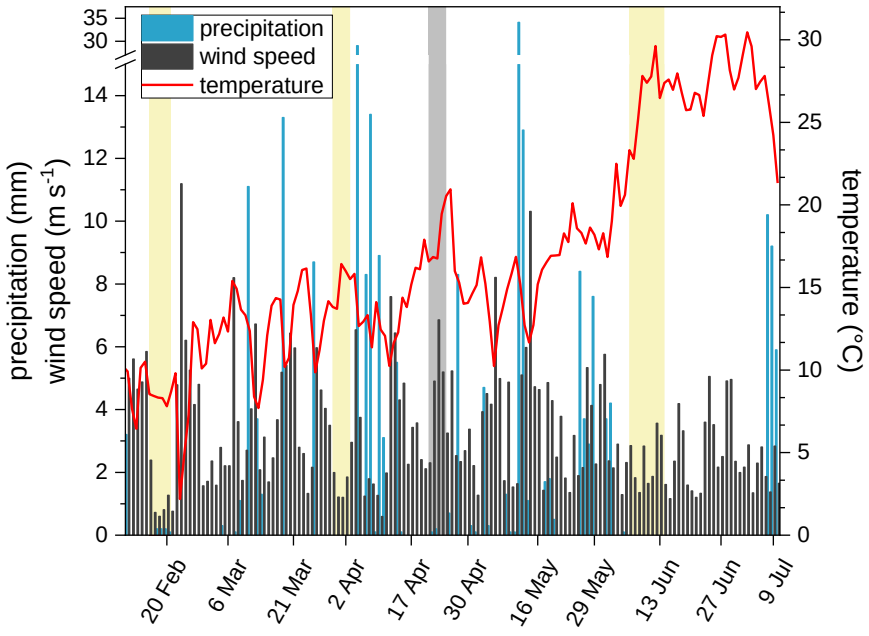

Fig. 2. Temporal variations of daily average meteorological parameters during the sampling campaign at the costal middle Adriatic site. The coloured vertical lines indicate the periods of open-fire BB (light yellow) and Saharan dust (light grey) events recorded during the sampling period.

Analysis of air-mass backward trajectory (AMBT) was performed using NOAA Hybrid Single Particle Lagrangian Integrated Trajectory Model (HYSPLIT), with Global Data Assimilation System (GDAS; 1 degree, global, 2006 – present) to differentiate between the main air-mass origins and long-range transport (Fig S1). Back-trajectories were calculated for 72-h time intervals with a 24-h frequency, which corresponds to three representative time points during the 48-h sampling period (beginning, middle, and end of the sampling time for each PM sample). The plots represent a trajectory ensemble of 3 single backward trajectories, ending at the sampling site at 5 m a.g.l.. Two source sectors were selected according to the dominant direction of the air-mass trajectory and its relative retention in the respective sectors: (a) marine sector - corresponding to marine air masses that spent most of their time over the open Adriatic Sea and/or Mediterranean Sea and (b) continental sector - corresponding to air masses that spent most of their time over the continental Europe (Figs. S1a and S1b). Samples not belonging to these groups were characterized as "undetermined" (mixed) cases (33% of the dataset) and were excluded from further discussion to provide unambiguous insight into the effects of contrasting long-distance source regions. The air masses reaching the middle Adriatic site during winter and early spring period (February – April) were predominantly from the continental sector, while the marine inflow significantly affected the area during late spring and summer period (May – July) (Fig. S2).

2.5. Specific events

Three intense open-fire BB events in winter (February 16th – 21st), spring (March 31st – April 2th) and summer (June 6th – 15th) were identified in the area according to AMBT analysis and Šibenik county fire department archive data (http://www.vatrogastvo-sibenik-knin.hr/, accessed January 20th, 2020), where compiled information on the intervention type (e.g., air-force intervention), fire duration, surface area attacked, and type of vegetation affected is registered. During the selected periods, intensive simultaneous and/or continuous open fires of grass, low plants, pine and olive tree forests were reported in the Šibenik county area within a radius of up to 20 km from the sampling location. The Saharan dust intrusion period was identified between April 21st – 25th according to AMBT analysis (Fig. S3).

2.6. Statistical analysis

The Shapiro-Wilk test was used to test the aerosol data for normality (n = 72, a = 0.05). Since the data were not normally distributed, Spearman's correlation coefficients were used to determine the correlations between aerosol data. Origin 7 (Origin Lab) and CorrData (https://sites.google.com/site/daromasoft/) softwares were used for statistical analysis. Kruskal-Wallis One-way analysis of variance (KW-ANOVA) was carried out to determine if there were significant differences between the variables.

3. **Results and discussion**

3.1. Variabilities of TM concentrations in atmospheric aerosols

The temporal distribution of TM concentrations in the PM_{10} samples collected at the middle Adriatic site in the period from February to July 2019 is presented in Fig. 3 while a statistical summary is shown in Table 1. The concentrations of investigated TMs in PM_{10} were of the order of magnitude found over remote western Mediterranean areas (Calzolai et al., 2015; Tovar-Sánchez et al., 2019b), but significantly lower compared to urban/industrial regions in the SE part of Italy (Contini et al., 2014), Greece (Manalis et al., 2005) as well as those measured in the northern Adriatic area (Contini et al., 2012, Toscano et al., 2011).

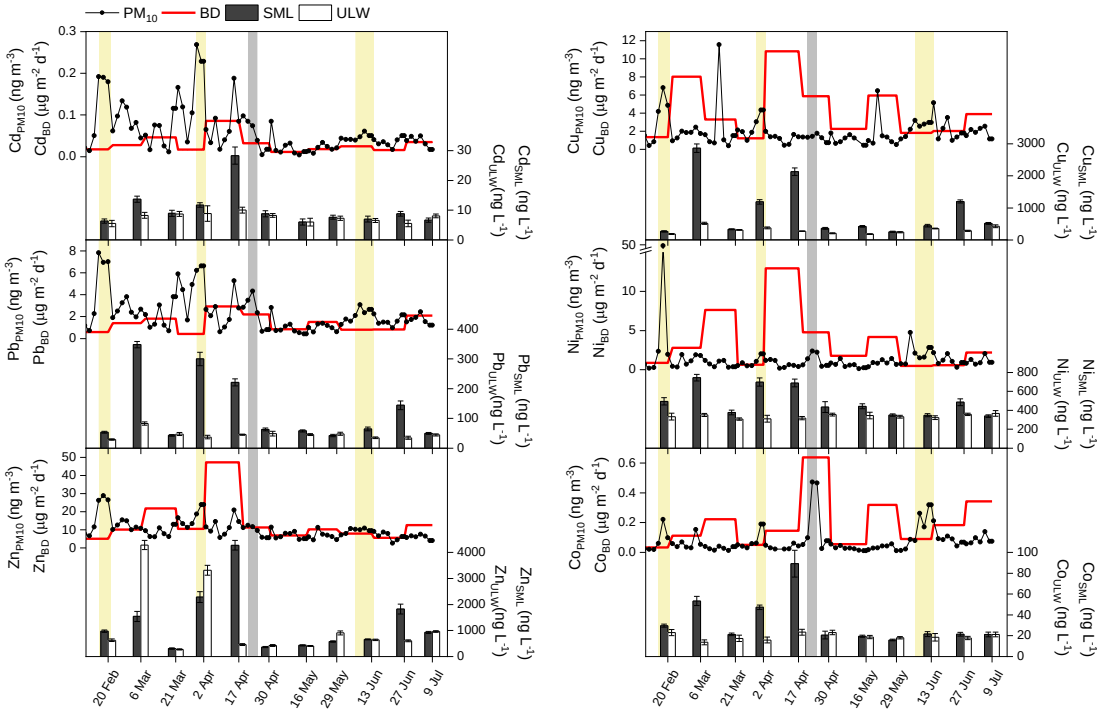

Fig. 3. Total concentrations of Cd, Cu, Pb, Ni, Zn, Co in PM_{10}, sea surface microlayer (SML), underlying water (ULW) and bulk deposition (BD) samples collected at the middle Adriatic site. The coloured vertical lines indicate periods of open-fire BB (light yellow) and Saharan dust (light grey) events recorded during the sampling period.

The concentrations of Zn, Cd and Pb were higher in the period between February and May and showed a strong mutual positive correlation (Table 2) which pointed to their common, anthropogenic origin (Birmili et al., 2006; Contini et al., 2012; Grgić et al., 2009; Manoli et al., 2002; Thurston et al., 2011). Indeed, considering the air-mass origins, concentrations of Zn, Cd and Pb in samples affected by the continental sector were significantly higher ($p < 0.05$) than those affected primarily by the marine inflow (Table 1), indicating more polluted continental impact in comparison to the southern marine inflows. The variable monthly contributions of continental and marine inflows (Fig. S2) showed that during the February – April period, when northern air-mass inputs dominated, anthropogenic emissions from industrial/urban activities in continental Europe can be treated as important factors affecting the concentrations of Zn, Cd and Pb at the middle Adriatic coastal area. It is worth noting that the world demand for Zn, Cu, Ni and Pb almost doubled between 2000 and 2020, indicating industrial activities as increasingly important sources of these elements (Watari et al., 2021).

Table 1 Average trace metal concentrations (ng m^{-3}) and standard deviation in PM_{10} samples and their distribution by dominant air-mass sectors and specific events (biomass burning BB; Saharan dust: SD) in comparison to the seasonal background levels at the middle Adriatic coastal site.

Overall	February–July	
Co	0.08±0.09	
Ni	1.09±0.77	
Cu	1.99±1.72	
Zn	10.08±5.34	
Cd	0.06±0.06	
Pb	2.35±1.72	
Air-mass sector	Continental (N, NW)	Marine (S, SE)
Co	0.07±0.05	0.10±0.14
Ni	1.21±1.02	1.26±0.72
Cu	2.68±2.4	2.14±1.63

Zn	14.16±5.84		8.67±4.39	
Cd	0.11±0.07		0.04±0.04	
Pb	3.72±1.92		1.93±1.48	
Seasonal background	Winter (Feb-Mar)	Spring (Apr-May)		Summer (Jun-Jul)
Co	0.05±0.03	0.03±0.02		0.09±0.04
Ni	0.88±0.52	0.72±0.38		1.38±1.08
Cu	2.03±2.2	1.32±1.13		2.09±1.08
Zn	11.06±3.57	8.46±3.84		6.68±2.07
Cd	0.08±0.04	0.04±0.04		0.04±0.01
Pb	2.71±1.43	1.49±1.11		1.67±0.39
Events	BB Winter	BB Spring	SD Spring	BB Summer
Co	0.13±0.08	0.13±0.09	0.35±0.21	0.21±0.11
Ni	2.15±0.27	1.55±0.68	2.00±0.54	2.00±0.61
Cu	5.28±1.36	3.67±0.92	1.50±0.23	2.85±0.28
Zn	27.14±1.39	21.2±3.67	11.2±1.45	10.14±0.61
Cd	0.19±0.01	0.25±0.03	0.07±0.02	0.05±0.01
Pb	7.26 ± 0.49	6.41 ± 0.28	3.39 ± 0.99	2.55 ± 0.42

The seasonal background distribution of Zn, Cd and Pb concentrations showed a decrease from winter towards spring and summer (Table 1), and a negative correlation with temperature (Table S3), indicating the impact of local/regional domestic heating activities on Zn, Cd and Pb levels during the cold period in this mostly rural area. A significant decrease in the concentrations of Zn, Cd and Pb was observed from end of April, when temperatures increased sharply and the dominance of marine air-mass inflow in the area occurred (Fig. S2),. The concentrations of Ni, Co and Cu showed a mutual, statistically significant positive correlation, but unlike Zn, Cd and Pb, were positively correlated with temperature, although statistically significant only for Co (Table S3). Moreover, their concentrations were slightly higher in summer than in winter, which was more pronounced in the case of Ni and Co. Ni, as one of the main impurities in heavy fuel oils, is considered a proxy for marine traffic emissions (Becagli et al., 2017), while the sources of Co include wind-blown dust, seawater spray, volcanoes, forest fires, fossil fuels, continental and marine biogenic emissions, industrial emissions, and Ni production (Barceloux, 1999; Crundwell et al., 2011; Kim et al., 2006). The potential source of atmospheric Cu, whose concentrations increased from spring towards summer, may have been brake abrasion from road traffic (Querol et al., 2007; Reizer et al., 2016), which is expected to increase during the summer

356 tourist season at the coastal Adriatic area. No significant difference in Ni, Co and Cu
357 concentrations was observed between the continental and marine air-mass sectors (Table 1),
358 implying that both long-range transport and/or local sources could influence their levels in PM_{10}
359 samples. Since the air masses from the marine sector dominated during the May – July period,
360 emissions from maritime transport could particularly affect Ni levels in the middle Adriatic
361 during the warmer tourist season. Indeed, a high influence of ship emissions originating from
362 both local harbours and maritime traffic across the Adriatic has been previously confirmed
363 (Bencardino et al., 2014).
364 To evaluate the impact of Saharan dust inputs and open-fire BB emissions in the area, average
365 TM concentrations in samples affected by these events were compared to the average
366 concentrations of corresponding seasonal background levels, considering only samples without
367 the special event inputs (Table 1). The intensive BB periods in winter, spring, and summer
368 caused considerable concentration increases of all TMs studied, especially during the winter
369 episode when all TMs showed a 2.5-fold increase, and during the spring episode when the TM
370 levels were from 2.2 times (Ni) to 6.3 times (Cd) higher compared to their average seasonal
371 background values. During the BB event in summer, Co showed the most significant increase,
372 approximately 2.4-fold above its summer seasonal background value. Numerous studies have
373 examined the effects of BB on ambient aerosol mass and ambient chemical composition (e.g.,
374 Chuang et al., 2013; Engling et al., 2009; Jaffe et al., 2008). Distinct regional characteristics of
375 BB smoke have been observed, suggesting that local BB emissions dominate aerosol chemistry,
376 while transport and mixing of BB aerosols from upwind sources are also common (e.g., Zhang
377 et al., 2012). Therefore, the TM levels in PM_{10} affected by emissions from open fires in different
378 seasons could be influenced by the combined effects of several factors such as fire intensity,
379 distance from the sampling site, the attacked surface area, type of burning material, and the
380 chemical and physical aging of the BB plumes (Hodshire et al., 2019).

381 Saharan dust intrusion in spring caused a considerable, 10-fold increase in Co concentration in
382 PM_{10} compared to respective background levels, confirming that dust intrusions are an
383 important Co source in addition to BB emissions (Almeida-Silva et al., 2013, 2014; Heimburger
384 et al., 2012).
385
386 3.2. Bulk deposition fluxes of TMs
387
406 Temporal variations of bulk TM deposition fluxes investigated at the middle Adriatic site
407 are shown in Fig. 3 while the data overview and comparison with other Mediterranean regions
408 are given in Table 2. Overall, 83% of the bulk deposition samples sustained at least one event
409 with more than 1 mm of precipitation, while only 2 dry periods were observed: February 20th –
410 March 5th and June 12th – 26th, 2019.
411 Zn exhibited the highest bulk deposition fluxes, followed by Cu and Ni. The determined values
412 were lower compared to north Adriatic Venice area, impacted by strong local and long-range
413 transport of anthropogenic emissions (Table 2) (Rossini et al., 2005). Compared to other
414 Mediterranean regions, bulk deposition fluxes of Cu and Zn at the middle Adriatic area were
415 similar, adding to the hypothesis of a uniformly polluted atmospheric background above the
416 Mediterranean (Guieu et al., 2010).
417
418 **Table 2** Bulk deposition flux ranges and averages (in parentheses) (μg m^{-2} d^{-1}) of analysed TMs
419 at the middle Adriatic coastal site, alongside those reported for other Mediterranean regions.
420

	Cd	Pb	Cu	Zn	Ni	Co
Middle Adriatic (2019)*	0.01–0.09 (0.03±0.02)	0.4–2.9 (1.4±0.8)	1.2–10.8 (4.2±3.1)	5.0–47.2 (13.5±12.1)	0.5–12.9 (3.5±3.8)	0.03–0.64 (0.20±0.18)
Middle Adriatic (1999-2004)[1]	0.08–0.6 (0.45±0.18)	7.9–14.9 (10.2±2.3)				
Middle Adriatic (1999-2004)[1]	0.10–0.63 (0.44±0.18)	2.5–6.2 (4.0±1.3)				

Corsica (2008-2011)[2]			(2.9±2.9)	(15.6±5.2)	(0.57±0.03)	
N Adriatic (1995-1996)[3]	(0.7±2.2)	(31.5±13.9)	(18.5±6.3)		(6.4±2.5)	
Venice (1993-1997)[3]	(0.60±0.30)	(57.5±23.3)	(30.9±5.7)		(9.5±1.1)	
Venice (1998-1999)[4]	(0.40±0.20)		(11.8±2.2)	(79.4±21.2)		
NE Greece (2001-2002)[5]	0.09	3.8		30.7		
S Greece (2001-2002)[5]	0.08	2.7		23.8		
S France (1991)[6]	(0.80–3.50)	8.8	7.4	5.4	2.5	0.10–1.10

*This study; [1]Čačković et al., 2009; [2]Desboueufs et al., 2018; [3]Rossini et al., 2001; [4]Rossini et al., 2005; [5]Guieu et al., 2010; [6]Guieu et al., 1997.

Bulk deposition fluxes of Cd (average 0.03 ± 0.02 μg m^{-2} d^{-1}) and Pb (average 1.41 ± 0.79 μg m^{-2} d^{-1}) were significantly lower compared to north Adriatic region. Comparison of the obtained TM deposition fluxes with a 6-year study performed in the period between 1999 and 2004 at the middle Adriatic coastal region (Čačković et al., 2009) indicated a substantial decrease in Pb and Cd, potentially due to the increased use of lead-free fuel and a reduction of industrial activities in the area.

Bulk TM deposition fluxes obtained at the coastal Adriatic area showed a high degree of variability, with specific periods contributing significantly to the overall bulk deposition fluxes of certain metals (Fig. 3). The Saharan dust event contributed between 8% of the total Zn and 29% of the total Co bulk deposition flux, while for other TMs (Cd, Pb, Cu and Ni) this event accounted on an average for 12% of the total bulk deposition flux. A single BB event in spring, coupled with several heavy rain events, also contributed strongly and caused a deposition maximum identified for all TMs except for Co; accounting for between 7% and 33% of the total Co and Ni bulk deposition fluxes respectively, and 25% of the total bulk deposition fluxes of Cd, Pb, Zn and Cu, respectively. The significance of wet deposition compared to dry deposition may change based on the removal efficiency of the two mechanisms and the local availability

of precipitation (Muezzinoglu and Cizmecioglu, 2006). For example, episodic wet deposition is considered the predominant removal mechanism for ecotoxicologically relevant metals in Germany at high latitudes (Gromping et al., 1997), whereas in semi-arid, Mediterranean regions with low precipitation, continuous dry deposition is most important on an annual basis (Grantz et al., 2003; Muezzinoglu and Cizmecioglu, 2006). Middle Adriatic is a watershed influenced by both Mediterranean and continental climate, with very little rain occurrences during the summer months. However, monthly averages can often be exceeded (Branković et al. 2013) and the analysis of annual precipitation in 2019 categorized the middle Adriatic area as wet to very wet (https://meteo.hr/klima_e.php?section=klima_pracenje&param=ocjena&MjesecSezona=godina&Godina=2019), indicating that precipitation may be an important pathway for the removal of atmospheric TMs at the coastal middle Adriatic area, as observed for other regions worldwide (Duce and Tindale, 1991; Spokes and Jickells, 2002). Indeed, statistically significant negative correlation between precipitation and aerosol concentrations of all TMs (Table S3) as well as the observed relationship between high bulk TM deposition fluxes and the highest precipitation amounts, indicated efficient TM removal from the atmosphere by wet deposition at the middle Adriatic area. However, our theoretical estimations of dry TM fluxes (Appendix S1) showed that dry TM deposition is also important for the investigated area, additionally confirming a high degree of uncertainty when a single fixed value for the dry deposition velocity (V_d) is used for the calculation. Therefore, future studies are necessary to more clearly distinguish between the specific contributions of wet and dry deposition in the area and their impact on the further cycling of TMs within the aquatic environment.

Compared to riverine inputs, the atmosphere is still a major source of TMs in the Mediterranean region, providing essential micronutrients for marine biochemical cycles (Guieu et al., 2010). This is especially relevant for the oligotrophic middle Adriatic where the pristine Krka River,

along with the karstic Zrmanja and Cetina Rivers present the only riverine inputs in this area. For comparison, one of the main sources of TMs in the north Adriatic is the Po River, accounting for approximately 40% of the total discharge of Adriatic rivers (Milliman et al., 2016). The ratio of atmospheric TM deposition (Table 2, North Adriatic, as reported by Rossini et al., 2001) and riverine TM input for the north Adriatic area of 25000 km^2 was calculated as 0.7 for Cd and Cu, and 2 for Pb (Rossini et al., 2001). Considering the TM input data of the Krka River (Cukrov et al., 2008), which were coupled with the atmospheric bulk TM deposition data in this work, the ratios of atmospheric TM deposition to Krka River TM input for the same surface were: 103, 339 and 604 for Cd, Cu and Pb, respectively. Although this is a rough estimate, it highlights the importance of atmospheric TM deposition and the necessity of investigating its biological impacts in the oligotrophic Adriatic region. In addition, occasional intense open-fire BB episodes and Saharan dust intrusions significantly affected bulk TM deposition, showing that even a small number of such extreme atmospheric events could provide a significant source of TMs and be responsible for most of the atmospheric deposition to the coastal water zones of the area.

3.3. Variabilities of TMs in the sea surface layers

The concentration ranges along with average values of the measured total and dissolved TMs in the SML and ULW are presented in Table 3, while the temporal distributions of the total TMs in the SML and ULW are given in Fig. 3. The concentrations of all measured dissolved and total TMs in SML and ULW are listed in Table S4. The highest concentrations in both total and dissolved fractions of the ULW were determined for Zn, followed by Ni, Cu, Pb, Co and Cd.

490

491 **Table 3** Total (T) and dissolved (D) TM concentrations and average values (in parentheses) (ng L^{-1}) in the SML and ULW at the middle Adriatic

492 coastal site, compared to values reported for other coastal regions.

Location		Cd	Pb	Cu	Zn	Ni	Co
SML							
Middle Adriatic*	T	6.0–28.3 (10.3±6.4)	42.8–348.1 (126.2±112.3)	251.3–2858.5 (904.5±868.7)	306.6–4274.9 (1287.7±1180.8)	339.4–744.2 (491.5±150.8)	15.9–89.1 (32.8±22.2)
Middle Adriatic*	D	5.2–9.6 (7.3±1.6)	21.9–38.8 (30.1±6.1)	151.1–1429.9 (517.2±392.3)	347.8–1261.7 (569.4±268.6)	237.9–402.7 (335.7±54.0)	7.4–23.2 (16.4±4.8)
Mediterranean area[1]	T	(24.0±6.0)	(1153.0±329.0)	(787.0±133.0)		(546.0±76.0)	(33.0±12.0)
NE Atlantic[1]	T	36.0±13.0	2333.0±811.0	7753.0±1843.0		276.0±59.0	16.0±9.0
Singapore[2]	T	20.0–80.0	110.0–510.0	1250.0–5720.0	5420.0–15370.0	460.0–2100.0	
S France[3]	D	8.5	94	1068	1000	199	13
Singapore[2]	D	20.0–50.0	20.0–120.0	270.0–720.0	1790.0–3310.0	310.0–500.0	
ULW							
Middle Adriatic*	T	5.5–10.0 (7.5±1.5)	29.4–82.7 (45.5±14.0)	180.8–517.2 (304.0±106.4)	273.7–4284.3 (1173.8±1332.2)	307.0–367.3 (336.7±20.2)	13.7–23.4 (19.2±3.2)
Middle Adriatic*	D	5.4–10.5 (7.4±2.0)	8.2–31.6 (23.6±6.9)	136.4–417.3 (232.3±79.3)	310.6–1294.1 (622.9±296.7)	231.6–336.8 (298.4±29.1)	15.7–19.9 (18.2±1.3)
Middle Adriatic[4]	T	7.8	20.9	228.7	340	437.2	21.2
NE Adriatic[5]	T	8.9–29.2	41–290	190.0–1270.0			
W Mediterranean[6]	T	(8.0±1.0)		(123.0±20.0)			(7.0±1.0)
E Mediterranean[6]	T	(10.0±1.0)		(133.0±11.0)			(9.0±3.0)
Middle Adriatic[4]	D	7.5	14.4	203.3	294.2	410.8	21.2
NE Adriatic[5]	D	7.6–28.1	18.0–82.0	127.0–699.0			
S Adriatic[7]	D	6.3–7.8	14.0–32.0	120.0–220.0	300.0–680.0	290.0–510.0	12.8–38.4
S France[8]	D	5.6–9.0	29.0–75.0	100.0–260.0	910.0–2020.0	330.0–580.0	13.0–59.0
W Med[9]	D	9.6	26	100	170	190	

*This study; [1]Tovar-Sánchez et al., 2019a; [2]Cuong et al., 2008 [3]Ebling and Landing 2015, [4]Cindrić et al., 2015; [5]Illuminati et al., 2019; [6]Tovar - Sanchez et al., 2014; [7]Cuculić et al., 2018; [8]Oursel et al., 2013; [9]Yoon et al., 1999.

The concentrations in the ULW were within expected ranges compared to surface layers in other Mediterranean areas, similar to those reported for the south Adriatic, but lower than those measured in the north Adriatic under the strong influence of Po River (Illuminati et al., 2019; Rossini et al., 2001). Total and dissolved Co, Pb and Cd concentrations in the ULW exhibited no clear temporal trends, while dissolved Cu and Zn concentrations showed a decrease from February/March to May, after which an increase was observed. Dissolved and total Ni showed a slight increase from late winter towards summer.

Concentrations of TMs in the SML showed much higher variability compared to the ULW, especially in the total fraction (Table 3, Fig. 3), indicating a higher variability of particulate matter associated TMs in the SML. The highest concentrations of both total and dissolved TMs in the SML were determined for Zn, followed by Cu, Ni, Pb, Co and Cd. Compared to other Mediterranean regions, the determined concentrations of dissolved and total TMs in the SML at the middle Adriatic coastal site were within the same orders of magnitude. Despite the high variability of total and dissolved TM concentrations in the SML, a general decrease in TM concentrations was observed from late winter towards summer, with an isolated increase on June 27th. However, dissolved Ni and Zn concentrations in the SML generally showed a slight increase for the same period. Statistically significant correlations between the SML and ULW total and dissolved TM concentrations were not found. It is expected that multiple physical, chemical and biological processes taking place in the SML could affect the partitioning and diffusion of TMs between sea surface compartments, which was observed by analysing the contributions of dissolved to total TM concentrations in the SML and ULW (Fig. 4). TMs in the ULW were mostly present in the dissolved fraction; on average, dissolved Cd, Ni and Co accounted for 89 ± 8%, Cu 79 ± 18%, Zn 69 ± 30% and Pb 54 ± 18% of the total fraction. Compared to the ULW, the average contributions of dissolved to total TM fraction were lower in the SML: 74 ± 23% for Cd and Ni, 66 ± 18% for Cu, 62 ± 32% for Zn, 58 ± 28% for Co and

520 43 ± 29% for Pb, stressing the importance of TM interaction with the particulate matter present
521 in the SML at the middle Adriatic coastal area, as recognized for other marine regions (Ebling
522 and Landing, 2015; Cuong et al., 2008, and references therein). With the exception of samples
523 impacted by BB events (see text below), the contributions of dissolved to the total TM fraction
524 in the SML were relatively high, especially in samples closely preceded by rain (e.g., late May
525 and early July), which were characterised by an overall decrease in aerosol TM concentrations
526 (Fig. 3), indicating efficient atmospheric TM partitioning and removal by wet deposition in the
527 coastal Adriatic area.
528

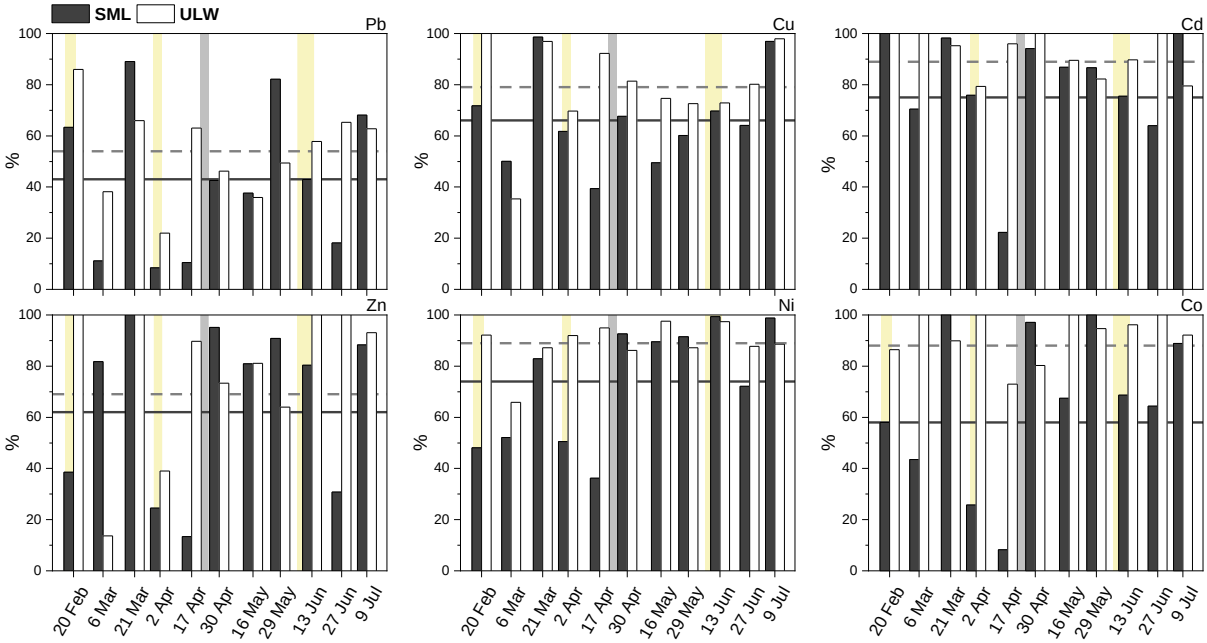

529
530
531 **Fig. 4.** Contribution of the TM dissolved fraction to the total TM concentrations determined in
532 the SML and ULW samples throughout the sampling campaign, capped at 100%. The coloured
533 vertical lines indicate periods of open-fire BB (light yellow) and Saharan dust (light grey)
534 events recorded during the sampling period. The horizontal lines present the average
535 contribution of each TM in the dissolved fraction of the SML (full grey line) and ULW (dashed
536 grey line), respectively.

Upon entering the aquatic environment, the dissolution of aerosol TMs is influenced by their origin and prior atmospheric processing, which affects their solubility and residence time (t_r) in the SML (Ebling and Landing, 2017; Mackey et al., 2015; Thuroczy et al., 2010). The t_r of the analysed TMs was determined using Eq. (1) (Chance et al., 2015; Ebling and Landing, 2017; Mohan, 2015)

$$t_r = [TM]_{SML} \times d / f_d \quad (1)$$

where $[TM]_{SML}$ is the total concentrations of TMs in the SML, d is the thickness of the SML, and f_d is the deposition flux of the aerosol TM, determined from the aerosol TM concentrations and the dry deposition velocity (V_d). However, instead of using a single fixed value of V_d to determine the residence time of TMs, Eq. (1) allowed the use of experimentally determined bulk deposition fluxes f_d (Appendix S1, Section 3.2.). Although dry deposition fluxes are commonly used, due to the fact that we only had two completely dry depositions, we believe that using bulk deposition fluxes that include both wet and dry deposition could provide a more realistic estimate of TMs residence times in the SML, despite the limitation of our ability to distinguish between the two deposition mechanisms. The t_r of the TMs showed high variability and ranged on average from 0.06 ± 0.05 h for Zn to 0.19 ± 0.08 h for Cd (Table 4). The values obtained were approximately an order of magnitude lower compared to values obtained for the open Mediterranean area (Tovar-Sánchez et al., 2019b) and fall between reported values for particulate and dissolved TM fractions (Ebling and Landing, 2017), indicating a combined influence of dissolved and particulate fractions on t_r.

Table 4 Calculated residence times (h) of analysed TMs and values reported in literature.

	Cd	Pb	Cu	Zn	Ni	Co
Total TM*	0.19±0.08	0.07±0.10	0.13±0.13	0.06±0.05	0.18±0.18	0.17±0.16
Total TM (Mediterranean)[1]		1.8±3.4	5.8±6.2	1.5±1.2	0.8±0.3	1.2±0.7
Particulate TM (Florida Keys)[2]		0.04–0.06	0.01–0.03	0.02–0.03	0.01–0.04	
Dissolved TM (Florida Keys)[2]		0.23–1.60	3.0–3.30	0.17–0.23	0.82–0.83	
Total TM (rural coastal areas)[3]		2.0	8.5	1.5	2.4	

*This study; [1]Tovar-Sanchez et al., 2019b, [2]Ebling and Landing, 2017, [3]Hardy et al., 1985a

Additionally, negative linear correlations determined among t_r of the analysed TMs, wind speed, and precipitation (Table S5), even though not statistically significant, suggested a potentially important role of meteorological conditions in considering the t_r of TMs in the SML, as shown previously (Hardy et al. 1985a).

Physical, chemical and biological characteristics of the receiving water system, such as the pre-existing concentrations of TMs and interactions with the particulate and dissolved OM, also influence their solubility, as well as bioavailability (Bruland et al., 1991; Sunda and Guilliard, 1976; Zhao et al., 2016). In the SML, POC and DOC concentrations ranged from 0.24 to 28.69 mg L^{-1} (average 3.53 ± 8.08 mg L^{-1}) and from 0.21 to 6.76 mg L^{-1} (average 1.47 ± 1.68 mg L^{-1}) respectively, with maximum values detected on April 2nd (Table S6). The percentage of all dissolved TMs in the SML lowered with increasing POC concentrations in the SML, which indicated an interaction between particulate OM and TMs, either by uptake/adsorption of TMs by microorganisms, or interaction with non-living particulate material. Concentrations of POC and DOC were significantly lower in the ULW, ranging from 0.09 to 0.31 mg L^{-1} (average 0.18 ± 0.07 mg L^{-1}) and from 0.79 to 0.97 mg L^{-1} (average 0.89 ± 0.07 mg L^{-1}), respectively. The observed relationship between dissolved Zn and POC concentrations in the SML and ULW illustrates the stark differences between the biogeochemical processes within these two

582 compartments. The decrease in the dissolved Zn concentrations in the ULW from February to
583 late April, followed by an increase towards June, suggested an uptake of Zn during late
584 winter/spring and subsequent release towards summer, reinforced by a negative linear
585 correlation, although not statistically significant, between dissolved Zn and POC concentrations
586 in the ULW ($r = -0.553$, $n = 11$; $p = 0.07$). Contrastingly, the correlation between dissolved Zn
587 and POC in the SML was highly positive and statistically significant ($r = 0.810$, $n = 10$, $p <$
588 0.05, extremely high POC value from April 2nd excluded from the analysis), indicating that
589 besides biological parameters, physico-chemical interactions strongly influence the distribution
590 of Zn at the air-water interface.
591 Accumulation of OM in the SML plays an important role in the enrichment of pollutants and
592 TMs within the SML, especially those that have a strong affinity for organic ligands (such as
593 Cu, Co, Cd, Fe) (Bruland and Lohan, 2006; Cunliffe and Murrell, 2009; Robinson et al., 2019;
594 Wurl and Obbard, 2004). The enrichment factor (EF), defined as the ratio of the respective
595 concentrations in the SML and ULW, shows that POC was enriched in all collected SML
596 samples, with the maximum EF determined on March 6th and April 2nd, when POC
597 concentrations in the SML were 63 and 263 times higher than in the ULW, respectively (Table
598 S6). Not considering these two sampling dates, the enrichment of total Pb, Zn, Cd, Co, Ni and
599 Cu (Fig. 5) showed significant positive linear correlations with the enrichment of POC ($r \geq$
600 0.87, $n = 9$, $p < 0.05$). The observed relationships could also have implications for TM
601 bioavailability, as TM interactions with OM, especially with the non-living organic particulates
602 within the SML, could mitigate the potentially toxic effects of elevated TM concentrations on
603 the microorganisms inhabiting the SML (Falkowska 1999, 2001; Hardy et al., 1985b; Lion and
604 Leckie, 1981).
605 The highest EF, determined for the total TM fraction, corresponded to the highest
606 concentrations of total TMs in the SML (Fig. 3), and followed a decreasing order: Pb > Cu >

607 Zn > Co > Ni > Cd, as predicted by Hardy et al. (1985a) for coastal environments. Average
608 enrichments of total TMs ranged from 1.4 for Cd to 3.2 for Pb and were highest in samples
609 collected after BB events.
610

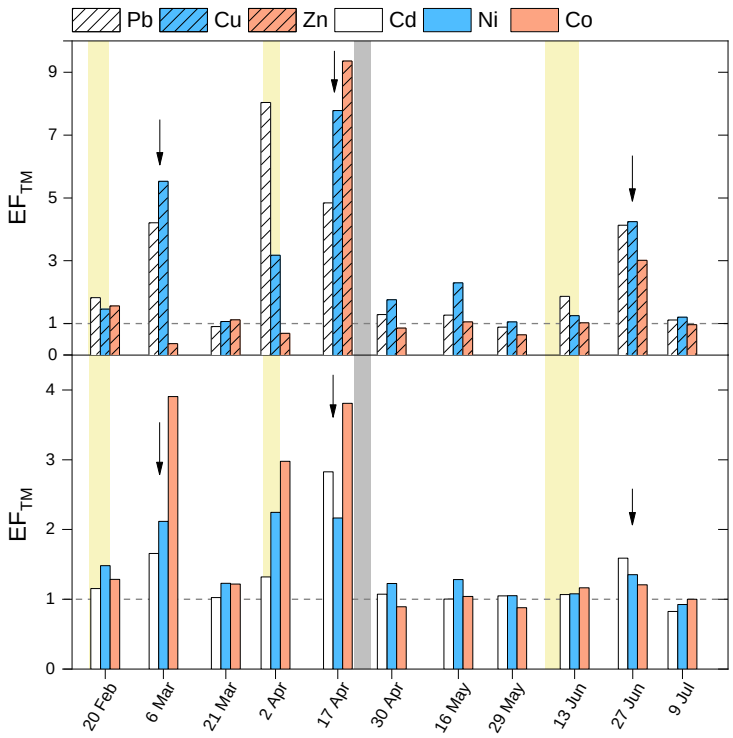

611

612 **Fig. 5.** Enrichment factors of total TMs in the SML: Pb, Cu, Zn, Cd, Ni and Co. The coloured
613 vertical lines indicate periods of biomass burning (light yellow) and Saharan dust events (light
614 grey) recorded during the sampling period. The arrows point to samples taken within two weeks
615 following a BB event.
616

617 The enrichment observed for the dissolved TM fraction was lower (Fig. S4) and ranged from
618 1.2 for Ni and Cd, to 2.5 for Cu, following the order: Cu > Pb ≈ Zn > Co ≈ Ni ≈ Cd. A
619 statistically significant positive linear correlation was found between dissolved Cu and DOC
620 enrichment factors ($r = 0.823$, $n = 10$, $p < 0.05$, extremely high DOC value from April 2nd
621 excluded from analysis). The observed correlation indicates the complexation of dissolved Cu

by dissolved OM (Coale and Bruland, 1990; Donat and van den Berg, 1992; Plavšić et al., 2009), with significant enrichment of dissolved Cu reported previously (Ebling and Landing, 2015).

3.4. Atmospheric deposition: impact of specific events on the TM levels in the SML

The middle Adriatic area is permanently exposed to from high to very high fire risk and has a long history of extreme forest fires. BB, including open vegetation fires and domestic heating is one of the largest sources of trace gases and aerosols to the global atmosphere (e.g. Andreae and Rosenfeld, 2008; Andreae, 2009; Crutzen and Andreae, 1990; Kaiser et al., 2012; van der Werf et al., 2017). The calculated average contribution of total Cu, Cd and Co in the SML to the uppermost meter of the surface waters, indicates how much TMs within the top meter of seawater was contained in the SML itself, and the average value of 0.004% obtained at the middle Adriatic coastal site is comparable to the study conducted along a west-east Mediterranean transect (Tovar-Sanchez et al., 2014). However, this average contribution increased 2-fold, to 0.009% following BB events in winter and spring, indicating the strong impact that BB could have on the biogeochemistry and the mass balance of the surface layers in the Mediterranean coastal areas. Intensive open-fire BB events in this study caused immediate significant increases in the concentrations of all TMs in aerosol samples, high bulk TM deposition fluxes (Fig. 3), and significant increases in total TM concentrations and enrichments of SML samples collected up to two weeks after BB events in winter, spring and summer (Fig. 5), implying a relationship between the intensive BB emission events and the TM concentrations in the SML. Since TMs are mostly associated with fine atmospheric particles that have the longest residence time in the atmosphere (up to several weeks), the observed increase in TM concentrations in SML samples collected up to two weeks after BB events could

be due to settling of atmospheric material. As the collected bulk deposition samples were collected continuously, unlike marine samples, over 12 – 16 days, and included both wet and dry deposition, we cannot discuss the exact contributions of the two different deposition mechanisms. However, wet removal dominates the atmospheric lifetime of pyrogenic particles, which is therefore largely controlled by meteorology (Garstang et al., 1997), and the highest TM deposition fluxes were generally related to high precipitation levels. The spring BB event was particularly interesting; a heavy rain period that followed caused the wash-out of aerosol TMs from the atmosphere, as indicated by the significant decrease of all TMs in the aerosols, the highest bulk deposition was observed for all TMs except Co (Fig. 2, Fig. 3), and the SML sample collected 2 weeks later had maximum enrichments of almost all TMs (Fig. 4). Compared to the solubility reported for different aerosol TMs (e.g. anthoropogenic, mineral dust) (Fishwick et al., 2018; López-Garcia et al., 2017; Mackey et al., 2015), the relative solubility of ash TM components from BB events can be up to two orders of magnitude lower: Ni 3.8%, Cu 0.5 – 13%, Zn 0.08%, Cd 0.2 – 2.8%, Pb 0.01 – 0.06% (Harper et al., 2019), which may in part explain the lower contribution of the dissolved fraction to total TM concentrations, especially in the case of Pb, even weeks after a fire event (Fig. 4). Contrarily, marine samples collected following rainy periods and without specific events showed a much higher contribution of the dissolved to the total TM fraction (Fig. 2, Fig. 4).

The interplay of various physical and chemical factors governs the fate of TMs in surface layers as well as their effects on the microbial community. The uptake and toxicity of TMs cannot be directly predicted by considering only the concentration of the free metal ion, as metal complexes have also been shown to contribute to metal bioavailability under certain conditions (Zhao et al., 2016). This is especially relevant to the SML, where TM accumulation of both the dissolved and particulate fraction has been observed, and physico-chemical reactions may have a greater impact on their speciation than in the ULW. For example, strong photooxidation of

672 OM to which the SML is exposed has been shown to reduce the complexing capacity of OM
673 (Sunda and Hanson, 1979), potentially leading to higher concentrations of the free ion or
674 smaller, labile organic complexes, which might facilitate higher TM bioavailability (Bruland et
675 al., 1991). Negative effects of TMs on marine organisms could also be enhanced in the SML
676 due to the synergistic effects of accumulated TMs (Thomas et al., 1980). Following BB events,
677 the SML contained on average 3.5 times more total TMs than the ULW while the enrichment
678 of TMs in the dissolved fraction was 1.6, with almost 5 times more dissolved Cu present in the
679 SML than in the ULW. Additionally, the average t_r of all total TMs determined in this study
680 doubled, increasing from 0.13 h to 0.25 h in samples following BB events. Thus, potentially
681 high negative impacts of TMs on the microbial community within the SML should be
682 considered, especially after intensive BB episodes, although the determined SML dissolved TM
683 concentrations were below the acute/chronic concentrations proposed for different TMs by
684 environmental protection agencies such as EPA (https://www.epa.gov/wqc/national-
685 recommended-water-quality-criteria-aquatic-life-criteria-table#a, accessed February 10th,
686 2021).
687 The Saharan dust intrusion was most evident in the significant increase in Co concentrations in
688 aerosols and subsequent bulk deposition samples. A number of studies have recognized the
689 importance and influence of Co as a limiting or co-limiting micronutrient for phytoplankton
690 dynamics in the open ocean (e.g., Bertrand et al., 2007; Panzeca et al., 2008; Saito et al., 2002,
691 2004, 2005; Saito and Goepfert, 2008). Saharan dust, almost continuously present in the
692 atmosphere above the Mediterranean Sea, but especially its strong plumes, may present an
693 important external TM source for the planktonic community of the Mediterranean Sea and can
694 impact primary production, especially in spring (Gallisai et al., 2014). The increase of Co in the
695 atmospheric samples was not followed by an increase of TM levels in the surface layers at the
696 coastal middle Adriatic site. There are several possible reasons for this: i) the intrusion itself

might not have been intense enough compared to other air-mass contributions that are continuously present in this coastal region, ii) the dust intrusion was not accompanied by strong precipitation that could have facilitated its deposition on the sea surface, iii) the material that deposited on the sea surface was removed by physical processes, while the dissolved Saharan dust Co, showing a wide range of solubility in seawater (Fishwich et al., 2018; Nimmo et al., 1998), might have been promptly processed by a microbial community prior to the next sampling. In addition to the nature and/or sources of aerosol material, the impact of atmospheric Co deposition on the dissolved Co budget is likely to be highly dependent on Co loading, as Co solubility could be inversely related to total Co loading (Chance et al., 2015) and finally iv) in contrast to BB material, the impact of specific mineral dust material on marine surface waters could be potentially underestimated due to the analysis protocol used for determination of the total TM concentrations in seawater samples, as it provides the acid-leachable TM or quasi-total TM concentration (see Section 2.2.1).

Our results confirmed that TM enrichment in the SML can be assigned as a first sentinel to increasing anthropogenic and natural impacts from the atmosphere on the ocean due to the rapid response in its physico-chemical features. Occasional environmental events such as intensive open-fire BB, dust influx or strong precipitation highly impacted the deposition of TMs to the sea surface as well as their biogeochemical cycling within the aquatic environment. Further research focused on better understanding the processes governing the biogeochemistry of TMs within the sea surface is needed, with a special emphasis on their impact on the aquatic biota, considering factors affecting their speciation and synergistic effects.

4. Conclusions

This study presents an integrated effort to assess the atmospheric deposition impacts of biologically relevant TMs (Zn, Cu, Co, Ni, Cd and Pb) on the sea surface of an oligotrophic coastal Mediterranean region, considering the SML at the air-water interface. The temporal distribution of TM concentrations in PM_{10} revealed that anthropogenic emissions from industrial/urban activities of continental Europe, along with local/regional domestic heating activities, can be treated as important factors affecting the concentrations of Zn, Cd and Pb, especially during winter – early spring. Intensive open-fire BB episodes in winter, spring and summer caused considerable concentration increase of all investigated TMs in the PM_{10} samples, while Saharan dust intrusion in spring caused a 10-fold increase in Co concentration compared to the respective background levels. Intensive BB events and Saharan dust intrusion also significantly affected the total bulk depositions of TMs. Compared to local riverine inputs, atmospheric deposition should be considered as a significant source of TMs in the shallow middle Adriatic coastal region, especially during periods of intensive emissions due to BB events and dust impacts. BB events, along with high precipitation, have been shown to significantly increase TM concentrations in the SML and impact TM partitioning in the surface waters. The significant enrichment of total TMs, as well as their longer residence time in the SML, observed in samples following BB episodes, could have implications for the bioavailability and toxicity of TMs to the microbial community inhabiting the SML.

Additionally, the high variabilities of TM concentrations observed within the SML sampled intensively over a six-month period indicated that special caution is required when designing field experiments, since the SML sampling on a one-time basis, e.g., during cruises, or occasional samplings within a particular season could result in capturing an unrepresentative snapshot of the situation and consequently lead to inaccurate conclusions with wide implications. Therefore, to better assess the cycling of TMs, but also of other biologically relevant compounds, through different environmental compartments, as well as to reconsider

746 the atmospheric impacts on the microbial community in oligotrophic marine environments,
747 intensive long-term studies employing the integrated approach are needed.
748
749 Acknowledgements
750
751 The financial support for this work was provided by BiREADI project (IP-2018-01-3105:
752 Biochemical responses of oligotrophic Adriatic surface ecosystems to atmospheric deposition
753 inputs; bireadi.irb.hr), funded by the Croatian Science Foundation.
754 The authors would like to acknowledge Dario Omanović for constructing the sea surface
755 microlayer sampler and making it available for this study. The authors would also like to thank
756 Zdeslav Zovko and Jelena Dautović for DOC and POC measurements, and along with Tomislav
757 Bulat, for their help during the field campaign.
758
759 **References**
760
761 Almeida-Silva, M., Almeida, S. M., Cardoso, J., Nunes, T., Reis, M. A., Chaves, P. C., Pio, C.
762 A., 2014. Characterization of the aeolian aerosol from Cape Verde by k0-INAA and
763 PIXE. J. Radioanal. Nucl. Chem. 300, 629–635. https://doi.org/10.1007/s10967-014-
764 2957-9.
765 Almeida-Silva, M., Almeida, S., M., Freitas, M. C., Pio, C. A., Nunes, T., Cardoso, J. 2013.
766 Impact of Sahara Dust Transport on Cape Verde Atmospheric Element Particles, J.
767 Toxicol. Environ. Health Part A. 76 (4-5), 240-251,
768 https://doi.org/10.1080/15287394.2013.757200.

769 Andreae, M., O., Rosenfeld, D., 2008. Aerosol–cloud–precipitation interactions. Part 1. The
770 nature and sources of cloud-active aerosol. Earth Sci. Rev. 89, 13-41.
771 https://doi.org/10.1016/j.earscirev.2008.03.001.
772 Andreae, M., O., 2009. Correlation between cloud condensation nuclei concentration and
773 aerosol optical thickness in remote and polluted regions, Atmospheric Chem. Phys. 9,
774 543–556. https://doi.org/10.5194/acp-9-543-2009
775 Barceloux, D., G., 1999. Cobalt. J. Toxicol. Clin. Toxicol. 37(2), 201–216.
776 https://doi.org/10.1081/CLT-100102420.
777 Baker, A., R., Thomas, M., Bange, H., W., Plasencia Sánchez, E., 2016. Soluble trace metals
778 in aerosols over the tropical south-east Pacific offshore of Peru. Biogeosciences. 13
779 817–825. https://doi.org/10.5194/bg-13-817-2016.
780 Bakšić, N., Vučetić, M., Španjol, Ž., 2015. Potencijalna opasnost od požara otvorenog prostora
781 u Republici Hrvatskoj. Vatrogastvo i upravljanje požarima. 5 (2), 30-40.
782 Becagli, S., Anello, F., Bommarito, C., Cassola, F., Calzolai, G., Di Iorio, T., di Sarra, A.,
783 Gómez-Amo, J.-L., Lucarelli, F., Marconi, M., Meloni, D., Monteleone, F., Nava, S.,
784 Pace, G., Severi, M., Sferlazzo, D. M., Traversi, R., Udisti, R., 2017. Constraining the
785 ship contribution to the aerosol of the central Mediterranean. Atmospheric Chem. Phys.
786 17(3), 2067–2084. https://doi.org/10.5194/acp-17-2067-2017.
787 Bencardino, M., M., Pirrone, N., N., Sprovieri, F., F., 2014. Aerosol and ozone observations
788 during six cruise campaigns across the Mediterranean basin: temporal, spatial, and
789 seasonal variability. Environ. Sci. Pollut. Res. Int. 21 (6), 4044-62.
790 https://doi.org/10.1007/s11356-013-2196-6.
791 Bertrand, E., M., Saito, M., A., Rose, M., J., Riesselman, C., R., Lohan, M., C., Noble, A., E.,
792 Lee, P., A., DiTullio, G., R., 2007. Vitamin B12 and iron co-limitation of phytoplankton

growth in the Ross Sea, Limnol. Oceanogr. 52, 1079–1093. https://doi.org/10.4319/lo.2007.52.3.1079.

Birmili, W., Allen, A. G., Bary, F., Harrison, R., M., 2006. Trace Metal Concentrations and Water Solubility in Size-Fractionated Atmospheric Particles and Influence of Road Traffic. Environ. Sci. Technol. 40 (4), 1144-53. https://doi.org/10.1021/es0486925.

Bonnet, S., Guieu, C., 2006. Atmospheric forcing on the annual iron cycle in the western Mediterranean Sea: A 1-year survey, J. Geophys. Res. Oceans. 111, C09010, https://doi.org/10.1029/2005JC003213.

Branković, Č., Güttler, I., Gajić-Čapka, M., 2013. Evaluating climate change at the Croatian Adriatic from observations and regional climate models' simulations. Clim. Dyn. 41, 2353–2373. https://doi.org/10.1007/s00382-012-1646-z.

Browning, T., J., Achterberg, E., P., Rapp, I., Engel, A., Bertrand, E., M., Tagliabue, A. Moore, C., M., 2017. Nutrient co-limitation at the boundary of an oceanic gyre. Nature. 551, 242-246. https://doi.org/10.1038/nature24063.

Bruland, K., W., Donat, J., R., Hutchins, D., A., 1991. Interactive influences of bioactive trace metals on biological production in oceanic waters. Limnol. Oceanogr. 36 (8), 1555-1577. https://doi.org/10.4319/lo.1991.36.8.1555.

Bruland, K., Lohan, M., C., 2006. Controls of Trace Metals in Seawater, In: Elderfield, H. (Ed.), Treatise on Geochemistry Series, Volume 6, Elsevier, Amsterdam, pp. 23-47.

Calzolai, G., Nava, S., Lucarelli, F., Chiari, M., Giannoni, M., Becagli, S., Traversi, R., Marconi, M., Frosini, D., Severi, M., Udisti, R., di Sarra, A., Pace, G., Meloni, D., Bommarito, C., Monteleone, F., Anello, F., Sferlazzo, D., M., 2015. Characterization of PM10 sources in the central Mediterranean. Atmospheric Chem. Phys. 15 (24), 13939–13955. https://doi.org/10.5194/acp-15-13939-2015.

817 Chance, R., Jickells, T., D., Baker, A., R., 2015. Atmospheric trace metal concentrations,
818 solubility and deposition fluxes in remote marine air over the south-east Atlantic.
819 Mar. Chem. 177 (1), 45-56. https://doi.org/10.1016/j.marchem.2015.06.028.
820 Chuang, M., Chou, C., Sopajaree, K., Lin, N., Wang, J., Sheu, G., Chang, Y., Lee, C., 2013.
821 Characterization of aerosol chemical properties from near-source biomass burning in
822 the northern Indochina during 7-SEAS/Dongsha experiment. Atmos. Environ. 78, 72-
823 81. https://doi.org/10.1016/J.ATMOSENV.2012.06.056.
824 Cindrić, A., M., Garnier, C., Oursel, B., Pižeta, I., Omanović, D., 2015. Evidencing the natural
825 and anthropogenic processes controlling trace metals dynamic in a highly stratified
826 estuary: The Krka River estuary (Adriatic, Croatia). Mar. Pollut. Bull. 94 (1–2), 199–
827 216. https://doi.org/10.1016/j.marpolbul.2015.02.029.
828 Contini, D., Belosi, F., Gambaro, A., Cesari, D., Stortini, A., M., Bove, M., C., 2012.
829 Comparison of PM10 concentrations and metal content in three different sites of the
830 Venice Lagoon: An analysis of possible aerosol sources. J. Environ. Sci. (China).
831 24(11), 1954–1965. https://doi.org/10.1016/S1001-0742(11)61027-9.
832 Contini, D., Cesari, D., Donateo, A., Chirizzi, D., Belosi, F., 2014. Characterization of
833 PM10 and PM2.5 and Their Metals Content in Different Typologies of Sites in South-
834 Eastern Italy. Atmosphere. 5(2), 435-453. https://doi.org/10.3390/atmos5020435.
835 Coale, K., H., Bruland, K., W., 1990. Spatial and temporal variability in copper complexation
836 in the North Pacific. Deep Sea Res. Part I Oceanogr. Res. Pap. 37 (2), 317–336.
837 https://doi.org/10.1016/0198-0149(90)90130-N.
838 Crundwell, F., K., Moats, M., S., Ramachandran, V., Robinson, T., G., Davenport, W., G.,
839 2011. Extractive metallurgy of nickel, cobalt and platinum group metals. Elsevier,
840 Oxford, UK. pp 315. https://doi.org/10.1016/B978-0-08-096809-4.10025-5.

841 Crutzen, P., J., Andreae, M., O., 1990. Biomass burning in the tropics: Impacton atmospheric
842 chemistry and biogeochemical cycles. Science. 250, 1669–1678.
843 https://doi.org/10.1126/science.250.4988.1669.
844 Cuculić, V., Cukrov, N., Kwokal, Ž., Strmečki, S., Plavšić, M., 2018. Assessing trace metal
845 contamination and organic matter in the brackish lakes as the major source of potable
846 water. Environ. Geochem. Health. 40, 489–503. https://doi.org/10.1007/s10653-017-
847 9935-4.
848 Cuculić, V., Cukrov, N., Kwokal, Ž., Mlakar, M., 2009. Natural and anthropogenic sources of
849 Hg, Cd, Pb, Cu and Zn in seawater and sediment of Mljet National Park, Croatia.
850 Estuar. Coast. Shelf Sci. 81 (3), 311-320. https://doi.org/10.1016/j.ecss.2008.11.006
851 Cukrov, N., Cmuk, P., Mlakar, M., Omanović, D., 2008. Spatial distribution of trace metals in
852 the Krka River, Croatia: An example of the self-purification. Chemosphere. 72 (10),
853 1559–1566. https://doi.org/10.1016/j.chemosphere.2008.04.038.
854 Cunliffe, M., Murrell, J., C., 2009. The sea-surface microlayer is a gelatinous biofilm. ISME J.
855 3, 1001-1003. https://doi.org/10.1038/ismej.2009.69.
856 Cunliffe, M., Upstill-Goddard, R., C., Murrel, J., C., 2010. Microbiology of aquatic surface
857 microlayer. FEMS Microbiol. Rev. 35, 233–246. https://doi.org/10.1111/j.1574-
858 6976.2010.00246.x.
859 Cunliffe, M., Engel, A., Frka, S., Gašparović, B., Guitart, C., Murrell, J., C., Salter, M., Stolle,
860 C., Upstill-Goddard, R., Wurl, O., 2013. Sea surface microlayers: A unified
861 physicochemical and biological perspective of the air-ocean interface. Prog. Oceanogr.
862 109, 104-116. https://doi.org/10.1016/j.pocean.2012.08.004.
863 Cuong, D., T., Karuppiah, S., Obbard, J., P., 2008. Distribution of heavy metals in the dissolved
864 and suspended phase of the sea-surface microlayer, seawater column and in sediments

865 of Singapore's coastal environment. Environ. Monit. Assess. 138, 255–272.
866 https://doi.org/10.1007/s10661-007-9795-y.
867 Čačković, M., Kalinić, N., Vadjić, V., Pehnec, G., 2009. Heavy metals and acidic components
868 in total deposited matter in Šibenik and National Park Kornati, Croatia. Arch. Environ.
869 Contam. Toxicol. 56(1), 12–20. https://doi.org/10.1007/s00244-008-9169-7.
870 Desboeufs, K., Bon Nguyen, E., Chevaillier, S., Triquet, S., Dulac, F., 2018. Fluxes and sources
871 of nutrient and trace metal atmospheric deposition in the northwestern Mediterranean.
872 Atmospheric Chem. Phys. 18 (19), 14477–14492. https://doi.org/10.5194/acp-18-
873 14477-2018.
874 Donat, J., R., van den Berg, C., M., G., 1992. A new cathodic stripping voltammetric method
875 for determining organic copper complexation in seawater. Mar. Chem. 38, 69–90.
876 https://doi.org/10.1016/0304-4203(92)90068-L.
877 Duce, A., R., Tindale, N., W., 1991. Atmospheric transport of iron and its deposition in the
878 ocean. Limnol. Oceanogr. 36 (8), 1715-1726.
879 https://doi.org/10.4319/lo.1991.36.8.1715.
880 Ebling, A., M., Landing, W., M., 2015. Sampling and analysis of the sea surface microlayer for
881 dissolved and particulate trace elements. Mar. Chem. 177, 134–142.
882 https://doi.org/10.1016/j.marchem.2015.03.012.
883 Ebling, A., M., Landing, W., M., 2017. Trace elements in the sea surface microlayer: Rapid
884 responses to changes in aerosol deposition. Elementa. 5: 42,
885 https://doi.org/10.1525/elementa.237.
886 Eker-Develi E., Kideys, A., E., Tugrul, S., 2006. Role of Saharan dust on phytoplankton
887 dynamics in the northeastern Mediterranean. Mar. Ecol. Prog. Ser. 314, 61–75.
888 https://doi.org/10.3354/meps314061.
889 Engel, A., Bange, H. W., Cunliffe, M., Burrows, S. M., Friedrichs, G., Galgani, L., Herrmann,

H., Hertkorn, N., Johnson, M., Liss, P., S., Quinn P., K., Schartau, M., Soloviev, A., Stolle, C., Upstill-Goddard, R., C., van Pinxteren, M., Zäncker, B., 2017. The ocean's vital skin: Toward an integrated understanding of the sea surface microlayer. Front. Mar. Sci. 4: 165, 1–14. https://doi.org/10.3389/fmars.2017.00165.

Engling, G., Lee, J., Tsai, Y.-W., Lung, S.-C.C., Chou, C.C.-K., Chan, C.-Y., 2009. Size resolved anhydrosugar composition in smoke aerosol from controlled field burning of rice straw. Aerosol Sci. Technol. 43, 662–672. https://doi.org/10.1080/02786820902825113.

Falkowska, L., 1999. Sea surface microlayer: A field evaluation of teflon plate, glass plate and screen sampling techniques. Part 2. Dissolved and suspended matter. Oceanologia. 41 (2), 223–240.

Falkowska, L., 2001. 12-hour cycle of matter transformation in the sea surface microlayer in the offshore waters of the Gdansk Basin (Baltic Sea) during spring. Oceanologia 43 (2), 201-222.

Fishwick, M., P., Ussher, S., Sedwick, P., Lohan, M., Worsfold, P., Buck, K., N., Church, T., 2018. Impact of surface ocean conditions and aerosol provenance on the dissolution of aerosol manganese, cobalt, nickel and lead in seawater. Mar. Chem. 198, 28-43. https://doi.org/10.1016/j.marchem.2017.11.003.

Gallisai, R., Peters, F., Volpe, G., Basart, S., Baldasano, J., M., 2014. Saharan Dust Deposition May Affect Phytoplankton Growth in the Mediterranean Sea at Ecological Time Scales. PLoS ONE. 9 (10): e110762. https://doi.org/10.1371/journal.pone.0110762.

Garstang, M., Tyson, P., D., Cachier, H., Radke, L., 1997. Atmospheric transport of particulate and gaseous products by fires, in: Sediment records of biomass burning and global change, vol. 51/Part III, Clark, J., S, Cachier, H., Goldammer, J. G., Stocks, B. (Eds.), Springer, Berlin Heidelberg New York, pp.207-252.

915 Grantz, D., A., Garner, J., H., B., Johnson, D., W., 2003. Ecological effects of particulate matter.
916 Environ. Int. 29 (2), 213-239. https://doi.org/10.1016/S0160-4120(02)00181-2.
917 Grgić, I., Turšič, J., Berner, A., 2009. Applying size segregation to relate the surrounding
918 aerosol pollution to its source. J. Atmos. Chem. 63 (3), 247–257.
919 https://doi.org/10.1007/s10874-010-9167-9.
920 Gromping, A., H., J., Ostapczuk, P., Emons, H., 1997. Wet deposition in Germany: Long–term
921 trends and the contribution of heavy metals. Chemosphere. 34 (9-19), 2227-2236.
922 https://doi.org/10.1016/S0045-6535(97)00080-5.
923 Gržetić, Z., Precali, R., Degobbis, D., Skrivanić, A., 1991. Nutrient enrichment and
924 phytoplankton response in an Adriatic karstic estuary. Mar. Chem. 32, 313-331.
925 https://doi.org/10.1016/0304-4203(91)90046-Y.
926 Guieu, C., Chester, R., Nimmo, M, Martin, J., M., Guerzoni, S., Nicholas, E., Mateu, J., Keyse,
927 S., 1997. Atmospheric input of dissolved and particulate metals to the northwestern
928 Mediterranean. Deep Sea Res. Pt. II. 44 (3-4), 655-674. https://doi.org/10.1016/S0967-
929 0645(97)88508-6.
930 Guieu, C., Ridame, C., Thomas, C., 2002. Chemical characterization of the Saharan dust end-
931 member: Some biogeochemical implications for the western Mediterranean Sea. J.
932 Geophys. Res. Atmos. 107 (D15), 4528. http:// doi.org/10.1029/2001JD000582.
933 Guieu, C., Loÿe-Pilot, M., D., Benyahya, L., Dufour, A., 2010. Spatial variability of
934 atmospheric fluxes of metals (Al, Fe, Cd, Zn and Pb) and phosphorus over the whole
935 Mediterranean from a one-year monitoring experiment: Biogeochemical implications.
936 Mar. Chem. 120 (1–4), 164–178.
937 https://doi.org/10.1016/j.marchem.2009.02.004.Guerzoni, S., Molinaroli, E., Chester,
938 R., 1997. Saharan dust inputs to the western Mediterranean Sea: depositional patterns,
939 geochemistry and sedimentological implications. Deep Sea Res. Pt. II., 64 (3-4), 631-

654. https://doi.org/10.1016/S0967-0645(96)00096-3.

Guerzoni, S., Chester, R., Dulac, F., Herut, B., Loye-Pilot, M.-D., Measures, C., Migon, C., Molinaroli, E., Moulin, C., Rossini, P., Saydam, C., Soudine, A., Ziveri, P., 1999. The role of atmospheric deposition in the biogeochemistry of the Mediterranean Sea. Prog. Oceanogr. 44, 147– 190. https://doi.org/10.1016/S0079-6611(99)00024-5.

Hardy, J., T., Apts, C., W., Crecelius, E., A., Fellingham, G., W., 1985a. The sea-surface microlayer: Fate and residence times of atmospheric metals. Limnol. Oceanogr. 30 (1), 93–101. https://doi.org/10.4319/lo.1985.30.1.0093.

Hardy, J., T., Apts, C., W., Crecelius, E., A., Bloom, N., S., 1985b. Sea surface microlayer enrichments in an urban and rural bay. Estuar. Coast. Shelf Sci. 20 (3), 299-312. https://doi.org/10.1016/0272-7714(85)90044-7.

Harper, A. R., Santin, C., Doerr, S. H., Froyd, C., A., Albini, D., Otero, X., L., Viñas, L., Perez-Férnández, B., 2019. Chemical composition of wildfire ash produced in contrasting ecosystems and its toxicity to Daphnia magna. Int. J. Widland Fire. 28, 726-787. https://doi.org/10.1071/WF18200.

Hassler, C., S., Sinoir, M., Clementson, L. A., & Butler, E. C. V., 2012. Exploring the link between micronutrients and phytoplankton in the Southern Ocean during the 2007 austral summer. Front. Microbiol. 3:202, 1–26. https://doi.org/10.3389/fmicb.2012.00202.

Heimburger, L.-E., Mignon, C., Dufour, A., Chiffoleau, J.-F., Cossa, D., 2010. Trace metal concentrations in the North-western Mediterranean atmospheric aerosol between 1986 and 2008: Seasonal patterns and decadal trends. Sci. Total Environ. 408, 2629–2638. https://doi.org/10.1016/j.scitotenv.2010.02.042.

964 Heimburger, L.-E., Losno, R., Triquet, S., Dulac, F., Mahowald, N., 2012. Direct measurements
965 of atmospheric iron, cobalt, and aluminum-derived dust deposition at Kerguelen Islands.
966 Global Biogeochem. Cycles. 26, GB4016.
967 https://doi.org/10.1029/2012GB004301.
968 Hodshire, A., L., Akherati, A., Alvarado, M., J., Brown-Steiner, B., Jathar, S., H., Jimenez, J.,
969 L., Kreidenweis, M., S., Lonsdale, C., R., Onasch, T., B., Ortega, A., M., Pierce, J., R.,
970 2019. Aging Effects on Biomass Burning Aerosol Mass and Composition: A Critical
971 Review of Field and Laboratory Studies. Environ. Sci. Technol. 53 (17), 10007-10022
972 https://doi.org/10.1021/acs.est.9b02588.
973 Hunter, K., A., Liss, P., S. (1981) Organic Sea Surface Films. In: Duursma, E., K. Dawson, R.,
974 (Eds.), Marine Organic Chemistry, Elsevier, New York, pp. 259-298.
975 https://doi.org/10.1016/S0422-9894(08)70331-3.
976 Illuminati, S., Annibaldi, A., Truzzi, C., Tercier-Waeber, M. Lou, Nöel, S., Braungardt, C.B.,
977 Achterberg, E.P., Howell, K.A., Turner, D., Marini, M., Romagnoli, T., Totti, C.,
978 Confalonieri, F., Graziottin, F., Buffle, J., Scarponi, G., 2019. In-situ trace metal (Cd,
979 Pb, Cu) speciation along the Po River plume (Northern Adriatic Sea) using submersible
980 systems. Mar. Chem. 212, 47-63. https://doi.org/10.1016/j.marchem.2019.04.001.
981 Jaffe, D., Hafner, W., Chand, D., Westerling, A., Spracklen, D., 2008. Interannual variations in
982 PM2.5 due to wildfires in the western United States. Environ. Sci. Technol. 42, 2812–
983 2818. https://doi.org/10.1021/es702755v.
984 Kaiser, J., W., Heil, A., Andreae, M., O., Benedetti, A., Chubarova, N., Jones, L., Morcrette,
985 J.-J., Razinger, M., Schultz, M., G., Suttie, M., and van der Werf, G., R., 2012. Biomass
986 burning emissions estimated with a global fire assimilation system based on observed
987 fire radiative power. Biogeosciences. 9, 527–554. https://doi.org/10.5194/bg-9-527-
988 2012.

989 Kanakidou, M., Mihalopoulos, N., Kindap, T., Im, U., Vrekoussis, M., Gerasopoulos, E.,
990 Dermitzaki, E., Unal, A., Koçak, M., Markakis, K., Melas, D., Kouvarakis, G., Youssef,
991 A., F., Richter, A., Hatzianastassiou, N., Hilboll, A., Ebojie, F., Wittrock, F., von
992 Savigny, C., Moubasher, H., 2011. Megacities as hot spots of air pollution in the East
993 Mediterranean. Atmos. Environ. 45 (6), 1223-1235.
994 https://doi.org/10.1016/j.atmosenv.2010.11.048.
995 Kim, J., H, Gibb, J., H, Howe, P., D., 2006. Cobalt and inorganic cobalt compounds. Concise
996 International Chemical Assessment Document 69. Geneva: World Health Organization.
997 Lee, J., G., Roberts, S., B., Morel, F., M., M., 1995. Cadmium: A nutrient for the marine diatom
998 Thalassiosira weissflogii. Limnol. Oceanogr. 40 (6), 1056–1063.
999 https://doi.org/10.4319/lo.1995.40.6.1056.
1000 Legović, T., Žutić, V., Grietif, Z., Cauwet, G., Precali, R., Viličić, D., 1994. Eutrophication in
1001 the Krka estuary. Mar. Chem. 46, 203-215. https://doi.org/10.1016/0304-
1002 4203(94)90056-6.
1003 Lion, L., W., Leckie, J., O., 1981. Chemical speciation of trace metals at the air-sea interface:
1004 The application of an equilibrium model. Environ. Geol. 3, 293–314.
1005 https://doi.org/10.1007/BF02473520.
1006 López-Garcia, P., Gelado-Caballero, M., D., Collado-Sánchez, C., Hernández-Brito, J., J.,
1007 2017. Solubility of aerosol trace elements: Sources and deposition fluxes in the Canary
1008 Region. Atmos. Environ. 148, 167-174.
1009 https://doi.org/10.1016/j.atmosenv.2016.10.035.
1010 Ljubešić, Z., Cetinić, I., Viličić, D., Mihalić, K., Caric, M., Olujić, G., 2007. Spatial and
1011 temporal distribution of phytoplankton in a highly stratified estuary (Zrmanja, Adriatic
1012 Sea). Mar. Ecol. 28, 169 - 177.
1013 https://doi.org/10.1111/j.1439-0485.2007.00180.x.

1014 Mackey, K., R., M., Chien, C.-T., Post, A., F., Saito, M., A., Paytan, A., 2015. Rapid and
1015 gradual modes of aerosol trace metal dissolution in seawater. Front. Microbiol. 5: 794,
1016 1-11. https://doi.org/10.3389/fmicb.2014.00794.
1017 Manalis, N, Grivas, G., Protonatoris, V., Moutsatsou, A., Samara, C., Chaloulakou, A., 2005.
1018 Toxic metal content of particulate matter (PM10), within the Greater Area of Athens.
1019 Chemosphere. 60 (4), 557-566. https://doi.org/10.1016/j.chemosphere.2005.01.003.
1020 Manoli, E., Voutsa, D., Samara, C., 2002. Chemical characterization and source identification/
1021 apportionment of fine and coarse air particles in Thessaloniki, Greece, Atmos. Environ.
1022 36, 949–961. https://doi.org/10.1016/S1352-2310(01)00486-1.
1023 Maranon, E., Behrenfeld, M., J., Gonzalez, N., Mourino, B., Zubkov, M., V., 2003. High
1024 variability of primary production in oligotrophic waters of the Atlantic Ocean:
1025 uncoupling from phytoplankton biomass and size structure, Mar. Ecol. Prog. Ser. 257,
1026 1-11. https://doi.org/10.3354/meps257001.
1027 Mahowald, N., M., Hamilton, D., S., Mackey, K., R., M., Moore, K., J., Baker, A., R., Scanza,
1028 R., A., Zhang, Y., 2018. Aerosol trace metal leaching and impacts on marine
1029 microorganisms. Nat. Commun. 9, 2614. https://doi.org/10.1038/s41467-018-04970-7.
1030 Milliman, J., D., Bonaldo, D., Carniel, S., 2016. Flux and fate of river-discharged sediments to
1031 the Adriatic Sea. Adv. Oceanogr. Limnol. 7 (2), 106-114.
1032 https://doi.org/10.4081/aiol.2016.5899.
1033 Migliavacca, M., Dosio, A., Camia, A., Hobourg, R., Houston-Durrant, T., Kaiser, J., W.,
1034 Khabarov, N., Krasovskii, A., A., Marcolla, B., San Miguel-Ayanz, J., Ward, D., S.,
1035 Cescatti, A., 2013. Modeling biomass burning and related carbon emissions during the
1036 21st century in Europe, J. Geophys. Res. Biogeosci., 118, 1732– 1747,
1037 https://doi.org/10.1002/2013JG002444.
1038 Mohan, M., S., 2015. An overview of particulate dry deposition: measuring methods, deposition

velocity and controlling factors. Int. J. Environ. Sci. Technol. 13, 387–402. https://doi.org/10.1007/s13762-015-0898-7.

Moulin, C., Lambert, C., Dulac, F. Dayan, U., 1997. Control of atmospheric export of dust from North Africa by the North Atlantic Oscillation. Nature. 387, 691–694. https://doi.org/10.1038/42679.

Morel, F., M., M., Price, N., M., 2003. The biogeochemical cycles of trace metals in the oceans. Science. 300 (5621), 944-947. https://doi.org/10.1126/science.1083545.

Muezzinoglu, A., Cizmecioglu, S., C., 2006. Deposition of heavy metals in a Mediterranean climate area. Atmos. Res. 81(1), 1–16. https://doi.org/10.1016/j.atmosres.2005.10.004.

Nimmo, M., Fon, G. R., Chester, R., 1998. Atmospheric deposition: A potential source of trace metal organic complexing ligands to the marine environment. Croat. Chem. Acta. 71 (2), 323-341.

Omanović, D., Kwokal, Ž., Goodwin, A., Lawrence, A., Banks, C. E., Compton, R. G., Komorsky-Lovrić, Š. 2006. Trace metal detection in Šibenik Bay, Croatia: Cadmium, lead and copper with anodic stripping voltammetry and manganese via sonoelectrochemistry. A case study. J. Iran. Chem. Soc. 3, 128-139. https://doi.org/10.1007/BF03245940.

Oursel, B., Garnier, C., Durrieu, G., Mounier, S., Omanović, D., Lucas, Y., 2013. Dynamics and fates of trace metals chronically input in a Mediterranean coastal zone impacted by a large urban area. Mar. Pollut. Bull. 69, 137–149. https://doi.org/10.1016/j.marpolbul.2013.01.023.

Panzeca, C., Beck, A., J., Leblanc, K., Taylor, G., T., Hutchins, D., A., Sañudo-Wilhelmy, S., A., 2008. Potential cobalt limitation of vitamin B12 synthesis in the North Atlantic Ocean, Global Biogeochem. Cycles. 22 (2), GB2029. https://doi.org/10.1029/2007GB003124.

1064 Pausas, J., G., Bladé, C., Valderantos, A., Seva, J., P., Fuentes D., Alloza J., A., Vilagros, A.,
1065 Bautista, S., Cortina, J., Vallejo, R., 2004. Pines and oaks in the restoration of
1066 Mediterranean landscapes of Spain: New perspectives for an old practice – a review.
1067 Plant. Ecol. 171, 209-220. https://doi.org/10.1023/B:VEGE.0000029381.63336.20.
1068 Plavšić, M., Gašparović, B., Strmečki, S., Vojvodić, V., Tepić, N., 2009. Copper complexing
1069 ligands and organic matter characterization in the northern Adriatic Sea. Estuar. Coast.
1070 Shelf Sci. 85, 299-306. https://doi.org/10.1016/j.ecss.2009.08.014.
1071 Querol, X., Alastuey, A., Moreno, T., Viana, M., Castillo, S., Pey, J., Escudero, M., Rodríguez,
1072 S., Cristóbal, A., González, A., Jiménez, S., Pallarés, M., de la Rosa, J., Artíñano, B.,
1073 Salvador, P., García Dos Santos, S., Fernández-Patier, R., Cuevas, E., 2007.
1074 Atmospheric particulate matter in Spain: levels, composition and source origin. In:
1075 EMEP Particulate Matter Assessment Report, EMEP/CCCReport 8/2007. Norwegian
1076 Institute for Air Research, Kjeller.
1077 Reizer, M., Juda-Rezler, K., 2016. Explaining the high PM10 concentrations observed in Polish
1078 urban areas. Air Qual. Atmos. Health. 9, 517-531.
1079 https://doi.org/10.1007/s11869-015-0358-z.
1080 Richon, C., Dutay, J.-C., Dulac, F., Wang, R., Balkanski, Y., Nabat, P., Aumont, O., Desboeufs,
1081 K., Laurent, B., Guieu, C., Raimbault, P., Beuvier, J., 2017. Modeling the impacts of
1082 atmospheric deposition of nitrogen and desert dust– derived phosphorus on nutrients
1083 and biological budgets of the Mediterranean Sea. Prog. Oceanogr. 163, 21-39.
1084 http://dx.doi.org/10.1016/j.pocean.2017.04.009.
1085 Richon, C., Dutay, J.-C., Dulac, F., Wang, R., Balkanski, Y., 2018. Modeling the
1086 biogeochemical impact of atmospheric phosphate deposition from desert dust and
1087 combustion sources to the Mediterranean Sea. Biogeosciences. 15, 2499-2524.
1088 http://dx.doi.org/10.5194/bg-15-2499-2018.

1089 Ridame, C., Guieu, C., Loÿe-Pilot, M.-D., 1999. Trend in total atmospheric deposition fluxes
1090 of Aluminium, iron and trace metals in the North western Mediterranean, over the past
1091 decade (1985-1997). J. Geophys. Res. Atmos. 104 (23). 30127-30138.
1092 https://doi.org/10.1029/1999JD900747.
1093 Robinson, T., B., Wurl, O., Bahlmann, E., Jürgens, K., Stolle, C., 2019. Rising bubbles enhance
1094 the gelatinous nature of the air–sea interface. Limnol. Oceanogr. 64 (6), 2358–2372.
1095 https://doi.org/10.1002/lno.11188.
1096 Rossini, P., Guerzoni, S., Rampazzo, G., Quarantatto, G., Garibbo, E., Molinaroli, E., 2001.
1097 Atmospheric Deposition of Trace Metals in North Adriatic Sea. In F. M. Faranda, L.
1098 Guglielmo and G. Spezie (Eds.). Mediterranean Ecosystems (pp. 123–129). Milan:
1099 Springer-Verlag. https://doi.org/10.1007/978-88-470-2105-1_17.
1100 Rossini, P., Guerzoni, S., Molinaroli, E., Rampazzo, G., De Lazzari, A., Zancanaro, A., 2005.
1101 Atmospheric bulk deposition to the lagoon of Venice: Part I. Fluxes of metals, nutrients
1102 and organic contaminants. Environ. Int. 31 (7), 959-974.
1103 https://doi.org/10.1016/j.envint.2005.05.006.
1104 Saito, M., A., Moffett, J., W., Chisholm, S., W., Waterbury, J., B., 2002. Cobalt limitation and
1105 uptake in Prochlorococcus. Limnol. Oceanogr. 47, 1629–1636.
1106 https://doi.org/10.4319/lo.2002.47.6.1629.
1107 Saito, M., A., Moffett, J., W., DiTullio, G., R., 2004. Cobalt and nickel in the Peru upwelling
1108 region: A major flux of labile cobalt utilized as a micronutrient. Global Biogeochem.
1109 Cycles. 18 (4), GB4030. https://doi.org/10.1029/2003GB002216.
1110 Saito, M., A., Rocap, G., Moffet, J., W., 2005. Production of cobalt binding ligands in a
1111 Synechococcus feature at the Costa Rica upwelling dome. Limnol. Oceanogr. 50, 279–
1112 290. https://doi.org/10.4319/lo.2005.50.1.0279.

1113 Saito, M., A., Goepfert, T., J., 2008. Zinc-cobalt colimitation of Phaeocystis antarctica, Limnol.
1114 Oceanogr. 53 (1), 266-275. https://doi.org/10.4319/lo.2008.53.1.0266.
1115 Siokou-Frangou, I., Christaki, U., Mazzocchi, M., G., Montresor, M., Ribera d'Alcalá, M.,
1116 Vaqué, D., Zingone, A., 2010. Plankton in the open Mediterranean Sea: a review.
1117 Biogeosciences. 7, 1543–1586. https://doi.org/10.5194/bg-7-1543-2010.
1118 Spokes, L., J., Jickells, T., D., 2002. Speciation of metals in the atmosphere. In: Chemical
1119 Speciation in the Environment, A. M. Ure, C. M. Davidson, (Eds.), pp 161–187.
1120 Blackwell Science Ltd, Oxford. https://doi.org/10.1002/9780470988312.ch7.
1121 Stolle, C., Ribas-Ribas, M., Badewien, T., H., Barnes, J., Carpenter, L., J., Chance, R.,
1122 Damgaard, L., R., Durán Quesada, A., M., Engel, A., Frka, S., Galgani, L., Gašparović,
1123 B., Gerriets, M., Hamizah Mustaffa, N., I., Herrmann, H., Kallajoki, L., Pereira, R.,
1124 Radach, F., Revsbech, N., P., Rickard, P., Saint, A., Salter, M., Striebel, M., Triesch,
1125 N., Uher, G., Upstill-Goddard, R., C., van Pinxteren, M., Zäncker, B., Zieger, P., Wurl,
1126 O., 2020. The MILAN Campaign: Studying Diel Light Effects on the Air–Sea Interface.
1127 Bull. Am. Meteorol. Soc. 101 (2), E146-E166. https://doi.org/10.1175/BAMS-D-17-
1128 0329.1.
1129 Sunda, W., Guillard, R., R., L., 1976. The relationship between cupric ion activity and the
1130 toxicity of copper to phytoplankton. J. Mar. Res. 34, 511-529.
1131 Sunda, W., G., Hanson, P., J., 1979. Chemical speciation of copper in river water. Effect of
1132 total copper, pH carbonate and dissolved organic matter. In: Chemical modeling in
1133 aqueous systems. E. A. Jenne (Ed), pp. 147-180. Vol. 93, ACS Symposium Series.
1134 Washington.
1135 Šiljković, Ž., Mamut, M., 2016. Forest fires in Dalmatia. Bulletin of Geography. Socio–
1136 economic Series. 32 (1), 117-130. https://doi.org/10.1515/bog-2016-0019.

1137 Toscano, G., Moret, I., Gambaro, A., Barbante, C., Capodaglio, G., 2011. Distribution and
1138 seasonal variability of trace elements in atmospheric particulate in the Venice Lagoon.
1139 Chemosphere. 85, 1518-1524. https://doi.org/10.1016/j.chemosphere.2011.09.045.
1140 Tovar-Sánchez, A., Arrieta, J., M., Duarte, C., M., Sañudo-Wilhelmy, S., A., 2014. Spatial
1141 gradients in trace metal concentrations in the surface microlayer of the Mediterranean
1142 Sea. Front. Mar. Sci. 1:79, 1-8. https://doi.org/10.3389/fmars.2014.00079.
1143 Tovar-Sánchez, A., González-Ortegón, E., & Duarte, C. M., 2019. Trace metal partitioning in
1144 the top meter of the ocean. Sci. Total Environ. 652, 907–914.
1145 https://doi.org/10.1016/j.scitotenv.2018.10.315.
1146 Tovar-Sánchez, A., Rodríguez-Romero, A., Engel, A., Zäncker, B., Fu, F., Marañón, E., Perez-
1147 Lorenzo, M., Bressac, M., Wagener, T., Desbouefs, K., Triquet, S., Siour, G., Guieu,
1148 C., 2019b. Characterising the surface microlayer in the Mediterranean Sea: trace metals
1149 concentration and microbial plankton abundance. Biogeosciences. 17 (8), 2349-2364.
1150 https://doi.org/10.5194/bg-17-2349-2020.
1151 Thomas, W., H., Hollibaugh, J., T., Seibert, D., L., R., Wallace Jr., G., T., 1980. Toxicity of a
1152 Mixture of Ten Metals to Phytoplankton. Mar. Ecol. Prog. Ser. 2 (3), 213-220.
1153 Thuroczy, C.-E., Boye, M., Losno, R., 2010. Dissolution of cobalt and zinc from natural and
1154 anthropogenic dusts in seawater. Biogeosciences. 7 (6), 1927–1936.
1155 https://doi.org/10.5194/bg-7-1927-2010.
1156 Thurston, G. D., Kazuhiko, I., Lall, R., 2011. A source apportionment of U.S. fine particulate
1157 matter air pollution. Atmos. Environ. 45 (24), 3924-3936.
1158 doi.org/10.1016/j.atmosenv.2011.04.070.
1159 van der Werf, G., R., Randerson, J., T., Giglio, L., van Leeuwen, T., T., Chen, Y., Rogers, B.,
1160 M., Mu, M., van Marle, M., J., E., Morton, D., C., Collatz, G., J., Yokelson, R., J.,

Kasibhatla, P., S., 2017. Global fire emissions estimates during 1997–2016. Earth Syst. Sci. Data. 9, 697–720. https://doi.org/10.5194/essd-9-697-2017.

Wurl, O., Obbard, J., P., 2004. A review of pollutants in the sea-surface microlayer (SML): A unique habitat for marine organisms. Mar. Pollut. Bull. 48 (11–12), 1016–1030. https://doi.org/10.1016/j.marpolbul.2004.03.016.

Watari, T., Nansai, K., Nakajima, K., 2021. Major metals demand, supply, and environmental impacts to 2100: A critical review. Resour. Conserv. Recycl. 164, 105107. https://doi.org/10.1016/j.resconrec.2020.105107.

Yoon, Y., Y., Martin, J., M., Cotté, M., H., 1999. Dissolved trace metals in the Western Mediterranean Sea: Total concentration and fraction isolated by C18 Sep-Pak technique. Mar. Chem. 66, 129–148. https://doi.org/10.1016/S0304-4203(99)00033-X.

Zhang, Y.-N., Zhang, Z.-S., Chan, C.-Y., Engling, G., Sang, X.-F., Shi, S., Wang, X.-M., 2012. Levoglucosan and carbonaceous species in the background aerosol of coastal southeast China: case study on transport of biomass burning smoke from the Philippines. Environ. Sci. Pollut. Res. 19 (1), 244-55. https://doi.org/10.1007/s11356-011-0548-7.

Zhao, C.-M., Campbell, P., G., C., Wilkinson, K., J., 2016. When are metal complexes bioavailable? Environ. Chem. 13, 425-433. http://dx.doi.org/10.1071/EN15205.

Supporting Information for the manuscript:

Atmospheric Deposition of Biologically Relevant Trace Metals in the Eastern Adriatic Coastal Area

Abra Penezić[a]*, Andrea Milinković[a], Saranda Bakija Alempijević[a], Silva Žužul[b], Sanja Frka[a]*

[a]Division for Marine and Environmental Research, Ruđer Bošković Institute, Zagreb, Croatia

[b]Institute for Medical Research and Occupational Health, Zagreb, Croatia

*Corresponding authors: abra@irb.hr; frka@irb.hr

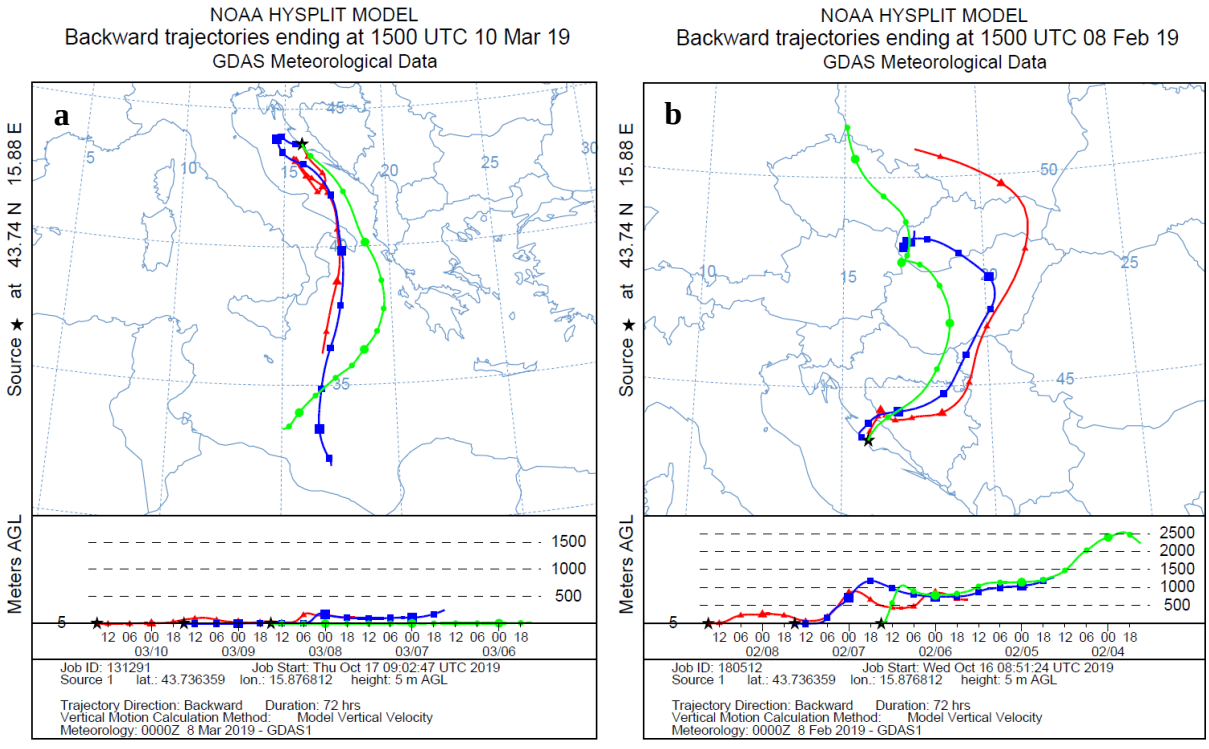

Fig. S1. Typical NOAA HYSPLIT air-mass backward trajectories of two dominant types of air masses ending up at the sampling site at the eastern middle Adriatic at 5 m a.g.l.: a) marine and b) continental.

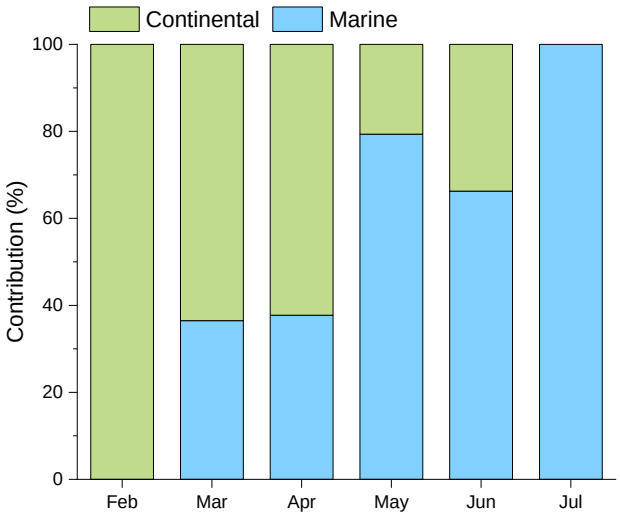

1202

1203 **Fig. S2.** Monthly variations in contribution of air-mass transport from contrasting northern
1204 continental (green bars) and southern marine (blue bars) sectors to the coastal middle Adriatic
1205 site, capped at 100%.

1206

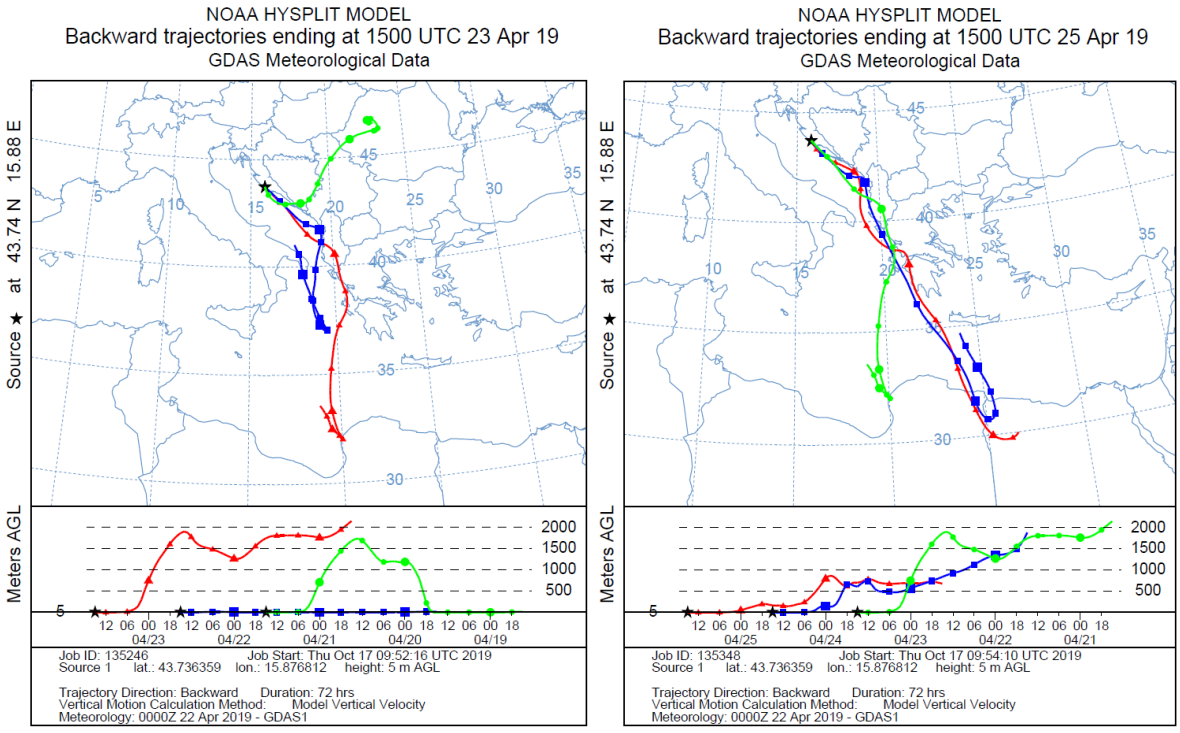

1207

1208 **Fig. S3.** NOAA HYSPLIT air-mass backward trajectories ending up at the sampling site at
1209 the eastern middle Adriatic at 5 m a.g.l in the period from April 21st to April 25th 2019.

Table S1 Experimental parameters for determination of TM concentration by differential pulse anodic stripping voltammetry (DPASV) and adsorptive cathodic stripping voltammetry (ACSV).

	DPASV				ACSV	
Parameter	Cd	Pb	Cu	Zn	Ni	Co
Deposition potential (V)	-0.85	-0.85	-0.85	-1.1	-0.7	-0.7
Modulation amplitude (V)	0.02	0.02	0.02	0.02	0.02	0.02
Step potential (V)	0.002	0.002	0.002	0.002	0.002	0.002
Deposition time (s)	600	600	600	120	120	120
Modulation time (s)	0.04	0.04	0.04	0.04	0.04	0.04
Interval time (s)	0.1	0.1	0.1	0.1	0.1	0.1

Table S2 Concentrations of TM determined for reference materials ERM CZ-120 (mg kg^{-1}), NIST 1648a (mg kg^{-1}), NASS6 (ng L^{-1}) (± present 95% confidence intervals for certified values and ± standard deviation for measured values).

Method			Cd	Pb	Cu	Zn	Ni	Co
ICP-MS	ERM CZ-120	certified	0.9 ± 0.2	113 ± 17	462	1240	58 ± 7	14.3
		measured	0.85 ± 0.04	109 ± 6	423 ± 18	1225 ± 39	57 ± 1	13.4 ± 0.5
	NIST 1648a	certified	73.7 ± 2.3	0.655 ± 0.033 %	610 ± 70	4800 ± 270	81.1 ± 6.8	17.9 ± 0.7
		measured	67.0 ± 1.1	0.668 ± 0.004 %	571 ± 4	4571 ± 59	75.7 ± 0.4	15.9 ± 0.1
DPASV ACSV	NASS-6	certified	31.1 ± 1.2	6 ± 2	248 ± 25	257 ± 20	301 ± 25	15
		measured	27.9 ± 3.8	8.3 ± 2.0	231 ± 18.3	258.2 ± 21.4	299.4 ± 36.8	15.5 ± 3.2

Table S3 Spearman's correlation matrix between the temperature (t), precipitation (prec) and trace metal concentrations in PM_{10} samples (n = 72) collected at the middle Adriatic sampling site. Statistically significant coefficients ($p < 0.05$) are marked bold.

	t	prec	Co	Ni	Cu	Zn	Cd	Pb
t	1	0.019	**0.387**	0.222	0.207	**-0.388**	**-0.285**	-0.164
prec		1	**-0.419**	**-0.323**	**-0.374**	**-0.303**	**-0.369**	**-0.375**
Co			1	**0.695**	**0.608**	**0.286**	**0.357**	**0.484**
Ni				1	**0.622**	**0.314**	**0.246**	**0.399**
Cu					1	**0.584**	**0.552**	**0.685**
Zn						1	**0.837**	**0.874**
Cd							1	**0.924**
Pb								1

1221

1222 **Table S4** Concentrations of total and dissolved TM (ng L^{-1}) determined with a 95% confidence interval in SML and ULW.

1223

	SML total											
date	Cd	±	Pb	±	Cu	±	Zn	±	Ni	±	Co	±
20.2.2019	6.35	0.72	53.69	3.32	264.20	24.70	973.24	43.80	494.89	37.80	29.66	1.44
6.3.2019	13.66	1.03	348.09	10.99	2858.47	132.84	1542.88	194.58	744.16	34.60	53.36	4.46
21.3.2019	8.93	1.03	43.17	2.59	330.81	14.45	306.61	23.70	377.70	23.93	21.33	1.19
2.4.2019	11.71	0.76	299.85	22.19	1185.59	70.96	2284.45	209.39	698.87	43.86	47.38	2.14
17.4.2019	28.31	2.86	221.11	12.07	2127.72	116.15	4274.88	183.50	688.55	40.52	89.14	12.85
30.4.2019	8.79	1.04	62.94	4.73	359.01	32.46	365.49	24.65	434.93	57.83	20.63	3.75
16.5.2019	6.01	1.04	58.15	3.42	419.63	27.12	431.41	23.37	442.98	26.41	19.47	0.99
29.5.2019	7.61	0.65	42.82	3.81	251.30	20.12	577.85	25.24	350.75	12.15	15.88	0.80
13.6.2019	6.98	0.99	64.76	6.01	440.94	39.78	659.37	18.98	348.69	15.52	21.57	2.41
27.6.2019	8.78	0.80	144.51	14.55	1199.29	45.93	1822.70	189.69	485.45	34.94	21.50	1.76
9.7.2019	6.64	0.72	49.65	3.39	512.83	28.44	925.80	38.66	339.38	13.59	21.24	2.34
	SML dissolved											
date	Cd	±	Pb	±	Cu	±	Zn	±	Ni	±	Co	±
20.2.2019	6.75	0.80	34.01	6.68	189.53	8.65	374.85	22.50	237.91	22.45	17.21	1.44
6.3.2019	9.62	1.03	38.80	3.17	1429.98	49.64	1261.67	71.39	387.51	42.79	23.23	3.00
21.3.2019	8.77	1.14	38.46	3.92	326.10	19.04	365.07	32.29	313.11	23.19	23.25	1.50
2.4.2019	8.88	0.64	25.11	1.81	731.95	31.31	559.21	47.81	352.97	19.74	12.19	1.36
17.4.2019	6.30	0.90	23.09	4.42	838.31	75.30	573.17	31.22	249.55	51.67	7.36	1.77
30.4.2019	8.27	0.86	26.80	3.31	242.72	13.96	347.78	12.99	402.74	24.16	20.04	1.67
16.5.2019	5.22	1.22	21.88	2.74	207.70	21.93	349.18	31.15	396.52	16.33	13.14	1.70
29.5.2019	6.59	0.80	35.18	3.31	151.08	26.96	525.08	15.93	320.87	23.12	16.98	1.16
13.6.2019	5.27	0.58	27.78	2.63	307.15	10.95	529.56	42.77	346.34	10.69	14.81	0.93
27.6.2019	5.62	0.43	26.24	1.59	767.96	71.02	560.70	16.27	350.10	19.03	13.83	0.98
9.7.2019	8.97	0.39	33.82	2.91	497.10	56.14	817.17	47.70	335.14	16.18	18.88	1.03

	ULW total											
date	Cd	±	Pb	±	Cu	±	Zn	±	Ni	±	Co	±
20.2.2019	5.50	1.07	29.41	2.53	180.78	13.69	624.15	50.25	333.74	36.41	23.07	2.95
6.3.2019	8.25	1.02	82.72	5.67	517.17	36.22	4284.34	179.20	351.53	16.13	13.66	2.37
21.3.2019	8.72	0.82	47.79	4.78	311.14	13.66	273.66	20.40	307.00	12.69	17.49	3.06
2.4.2019	8.87	2.62	37.30	5.90	373.66	27.22	3315.20	190.01	311.21	35.63	15.91	2.75
17.4.2019	10.01	0.98	45.66	1.91	273.39	8.78	456.67	35.68	318.11	17.37	23.40	2.88
30.4.2019	8.20	0.62	48.87	7.88	204.19	15.15	427.06	37.12	354.37	15.21	23.09	2.08
16.5.2019	5.99	1.30	45.90	3.24	182.73	10.62	409.83	18.46	345.12	33.69	18.72	1.56
29.5.2019	7.26	0.73	48.37	5.02	239.04	17.87	907.66	77.99	333.55	14.92	18.06	1.22
13.6.2019	6.53	0.69	34.78	2.75	353.58	10.11	643.67	27.65	323.08	19.78	18.52	3.61
27.6.2019	5.52	1.09	34.98	5.17	282.66	18.34	605.44	33.29	358.47	12.47	17.82	1.55
9.7.2019	8.05	0.61	44.64	3.20	425.90	47.28	964.34	33.26	367.28	29.21	21.23	2.32
	ULW dissolved											
date	Cd	±	Pb	±	Cu	±	Zn	±	Ni	±	Co	±
20.2.2019	6.35	1.06	25.28	3.32	181.22	20.04	741.95	41.32	307.45	12.49	19.93	1.12
6.3.2019	10.51	2.18	31.59	3.46	182.80	13.30	586.31	20.29	231.60	34.49	17.58	1.66
21.3.2019	8.30	0.84	31.52	2.52	301.58	9.20	310.57	16.55	267.68	11.10	15.73	1.98
2.4.2019	7.04	1.81	8.19	1.95	260.31	9.79	1294.06	89.06	286.24	22.04	19.40	2.08
17.4.2019	9.61	1.22	28.78	4.82	252.22	18.01	409.47	19.34	301.93	17.22	17.07	2.05
30.4.2019	10.48	0.87	22.58	3.22	166.23	11.48	313.32	23.51	305.17	16.57	18.54	1.12
16.5.2019	5.36	0.96	16.49	1.05	136.38	11.88	332.36	14.04	336.78	16.58	19.34	1.19
29.5.2019	5.97	0.38	23.88	1.40	173.51	6.44	580.53	35.63	290.88	9.49	17.10	1.41
13.6.2019	5.86	0.47	20.12	1.55	257.54	13.13	646.12	39.52	314.51	12.82	17.81	2.32
27.6.2019	5.53	1.04	22.83	2.18	226.56	14.88	739.28	37.08	314.50	12.30	18.57	1.80
9.7.2019	6.40	0.80	28.02	1.65	417.33	29.97	897.44	36.02	325.35	14.97	19.56	2.05

1224

1225

Table S5 Pearson's correlation matrix between the wind speed (WS), precipitation (prec) and residence time of trace metals (n=11) collected at the middle Adriatic sampling site. Statistically significant coefficients, at a 95% confidence interval, are marked bold.

	WS	prec	Cd	Pb	Cu	Zn	Ni	Co
WS	1	0.417	-0.585	**-0.645**	**-0.642**	-0.517	-0.332	-0.437
prec		1	-0.482	-0.495	-0.568	**-0.72**	**-0.707**	-0.326
Cd			1	**0.757**	**0.795**	**0.679**	**0.658**	0.485
Pb				1	**0.931**	0.565	**0.737**	**0.645**
Cu					1	**0.774**	**0.867**	0.534
Zn						1	**0.800**	0.398
Ni							1	0.497
Co								1

Table S6 Concentrations of dissolved (DOC) and particulate (POC) organic carbon (mg L^{-1}) determined in SML and ULW, and their enrichment factors (EF).

	POC			DOC		
date	SML	ULW	EF	SML	ULW	EF
20.2.2019	0.25	0.10	2.5	0.79	0.81	1.0
6.3.2019	5.66	0.09	62.9	1.52	0.79	1.9
21.3.2019	0.24	0.16	1.5	0.88	0.85	1.0
2.4.2019	28.69	0.11	263.2	6.76	0.97	7.0
17.4.2019	2.88	0.21	13.8	1.16	0.97	1.2
30.4.2019	0.69	0.31	2.2	1.03	0.97	1.1
16.5.2019	0.29	0.23	1.3	1.00	0.97	1.0
29.5.2019	0.49	0.21	2.3	0.42	0.90	0.5
13.6.2019	0.50	0.28	1.8	0.67	0.94	0.7
27.6.2019	1.55	0.19	8.0	0.92	0.84	1.1
9.7.2019	0.26	0.14	1.9	0.21	0.90	0.2

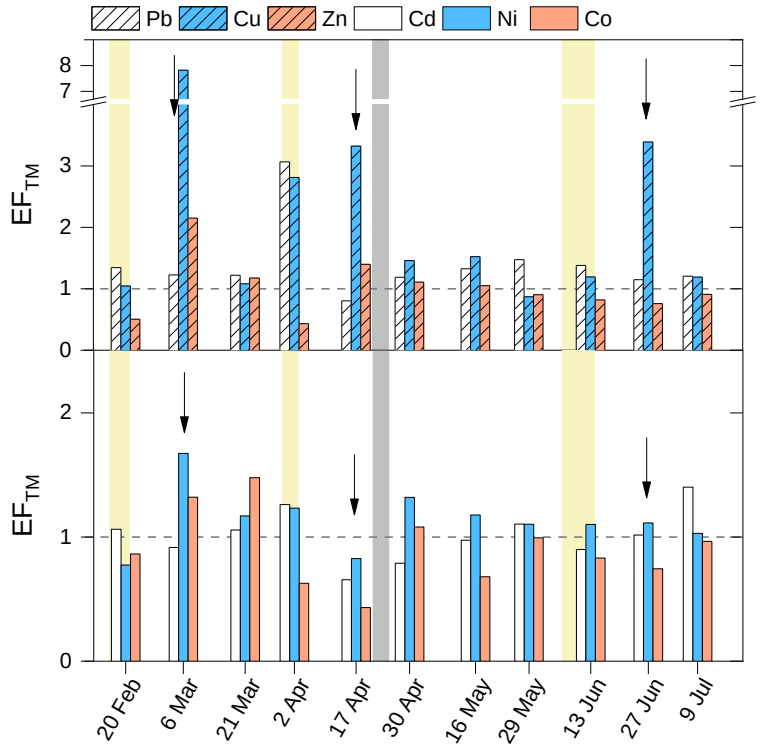

Fig. S4. Enrichment factors of dissolved TM: Pb (white striped bar), Cu (blue striped bar), Zn (red striped bar), Cd (white bar), Ni (blue bar) and Co (red bar). The coloured vertical lines indicate biomass burning (light yellow) and Saharan dust (gray) events recorded during the sampling period. The arrows point to samples taken within two weeks following a BB event.

Appendix S1

Dry vs. wet deposition

To assess to which extent the dry deposition flux contributed to the total deposition flux, the dry deposition fluxes (f_d) of particular TM (µg m^{-2} d^{-1}) were calculated by using the following equation (Chance et al., 2015; Mohan et al., 2016):

$f_d = C \times V_d$ (1)

Here, C is the biweekly average aerosol TM concentration (µg m^{-3}) and V_d is dry deposition velocity (cm s^{-1}). Processes that control V_d include gravitational settling, impaction, and diffusion. These processes act simultaneously and are affected by many variables including

particle size, wind speed, relative humidity, and sea surface roughness. Owing to the absence of experimentally determined deposition rates and aerosol size distribution, the estimation of f_d by using a single species-specific V_d value reported in the literature is still standard. Thus, the literature value of 0.3 cm s^{-1} was used in this work for the estimation of dry deposition fluxes of TM studied, reflecting their association with fine aerosol particles (Baker et al., 2016; Duce et al., 1991; Herut et al., 2001). On average, dry deposition fluxes calculated following the above approach contributed to total bulk deposition by 17±14% for Co, 20±16% for Cu, 29±21% for Zn, 42±68% for Ni, 69±80% for Pb and 71±57% for Cd.

The comparison of calculated dry deposition and actually measured bulk deposition in the case of two bulk deposition samples which did not include any precipitation events – that is, the contribution of the calculated dry to the measured dry deposition flux is expected to be around 100%, pointed to a large underestimation of the calculated dry deposition fluxes of TM at the coastal middle Adriatic. For the two dry samples, the calculated dry deposition fluxes contributed to the measured deposition flux by respectively: 15% and 19% for Co, 6% and 32% for Cu, 31% and 33% for Zn, 11% and 68% for Ni, 48% and 52% for Pb and 99% and 58% for Cd. Such underestimation and variability stem from several factors. Firstly, both dry periods demonstrate potentially important variability driven by the occurrence of biomass burning events which in turn could influence their coarse-to-fine aerosol ratio and consequently cause their variable deposition velocities (Sakata and Marumoto, 2004). Secondly, atmospheric deposition collection efficiency during dry periods could be largely affected by the collector geometry and the surface characteristics (Dasch, 1985; Shannigrahi et al., 2005). Additionally, the dry flux calculated by using Eq. 1 does not include TM originating from the total atmospheric material, but only particles with a diameter of 10 μm and less. Considering another approach, Eq. 1 also enabled us to determine the V_d for the 6 analysed TMs by using the

measured dry deposition flux in the case of the two dry samples collected, and the concentration of TMs in PM_{10} samples:

$$V_d = f_d / C \qquad (2)$$

The obtained values were comparable to those obtained by Sakata et al. (Sakata and Marumoto, 2004, Sakata et al., 2008) (**Table S1.1**) and are mainly above 0.3 cm s^{-1}, with an average value of 1.4 cm s^{-1}.

Table S1.1 Deposition velocities (cm s^{-1}) calculated for bulk deposition samples collected during two dry periods at the middle Adriatic coastal area.

Deposition velocity	Cd	Pb	Cu	Zn	Ni	Co
February/March 2019, PM_{10}	0.3	0.6	5.4	1.0	2.7	2.1
July 2019, PM_{10}	0.5	0.6	0.9	0.9	0.4	1.6

These calculations highlight the underestimation/uncertainty in the dry deposition flux calculation of TM if one single fixed value of V_d is used.

1293 References

1294

1295 Dasch, J., M., 1985. The direct measurement of dry deposition to a polyethylene bucket and
1296 various surrogate surfaces. Environ. Sci. Technol. 19, 721-5.
1297 https://doi.org/10.1021/es00138a011.

1298 Duce, R., A., Liss, P., S., Merrill, J., T., Atlas, E., L., Buat-Menard, P., Hicks, B., B, Miller, J.,
1299 M., Prospero, J., M., Arimoto, R., Church, T., M., Ellis, W., Galloway, J., N., Hanse,
1300 L., Jickells, T., D., Knap, A., H., Reinhardt, K., H., Schneider, B., Soudine, A., Tokos,
1301 J., J., Tsunogai, S., Wollast, R., Zhou, M., 1991. The atmospheric input of trace species
1302 to the world ocean. Global Biogeochem. Cycles. 5(3), 193-259.

1303 Herut, B., Nimmo, M., Medway, A., Chester, R., Krom, M., D., 2001. Dry atmospheric inputs
1304 of trace metals at the Mediterranean coast of Israel (SE Mediterranean): sources and
1305 fluxes. Atmos. Environ. 35 (4), 803-813. https://doi.org/10.1016/S1352-
1306 2310(00)00216-8.

1307 Sakata, M., Marumoto, K., 2004. Dry Deposition Fluxes and Deposition Velocities of Trace
1308 Metals in the Tokyo Metropolitan Area Measured with a Water Surface Sampler.
1309 Environ. Sci. Technol. 38, 2190-2197. https://doi.org/10.1021/es030467k.

1310 Sakata, M., Tani, Y., Takagi, T., 2008. Wet and dry deposition fluxes of trace elements in Tokyo
1311 Bay. Atmos. Environ. 42 (23), 5913–5922.
1312 https://doi.org/10.1016/j.atmosenv.2008.03.027.

1313 Shannigrahi, A., S., Fukushima, T., Ozaki, N., 2005. Comparison of different methods for
1314 measuring dry deposition fluxes of particulate matter and polycyclic aromatic
1315 hydrocarbons (PAHs) in the ambient air. Atmos. Environ. 39 (4), 653-662.
1316 https://doi.org/10.1016/j.atmosenv.2004.10.025.

1317